ELSEVIER

Contents lists available at ScienceDirect

### Journal of Hydrology

journal homepage: www.elsevier.com/locate/jhydrol



#### Research papers

## Intermittent viscous debris flow formation in Jiangjia Gully from the perspectives of hydrological processes and material supply



Xiaojun Guo<sup>a,b,\*</sup>, Yong Li<sup>a</sup>, Peng Cui<sup>a,b</sup>, Hua Yan<sup>a,c</sup>, Jianqi Zhuang<sup>d</sup>

- a Key Laboratory of Mountain Hazards and Surface Process/Institute of Mountain Hazards and Environment, Chinese Academy of Sciences, Chengdu 610041, China
- <sup>b</sup> CAS Center for Excellence in Tibetan Plateau Earth Sciences, Beijing 100101, China
- <sup>c</sup> University of Chinese Academy of Science, Beijing 100039, China
- <sup>d</sup> School of Geological Engineering and Surveying, Changan University, Xi'an 710064, China

#### ARTICLE INFO

# Keywords: Debris flow Formation process Slope failure Rainfall condition Jiangjia Gully

#### ABSTRACT

Debris flows are among the most destructive natural processes to affect areas of mountainous terrain. Debris flow formation involves watershed-scale processes of hydrology and material supply. This study explored both processes based on long-term monitoring data from the Jiangjia Gully in southwestern China. Based on hydrological simulations, we found that the debris flows formed as "normal" or "abnormal" hydrological processes. The former, with normal time lag  $\tau$  and normal peak discharge  $Q_{\rm max}$ , formed as a typical hydrological process in which slope failure material was mixed instantaneously with channel runoff. Conversely, the latter, with longer time lag  $\tau$  and/or abnormal discharge  $Q_{\rm max}$ , formed through blockage and outburst associated with landslides. We found that the different types of debris flow required similar rainfall conditions and that the threshold could be expressed as  $I=6.25\,D^{-0.73}$  ( $0.5 \le D \le 14.5\,h$ ). Furthermore, we established that rainfall pattern influences debris flow occurrence, that is, such events are more likely during short-duration rainfall. The findings of this study highlight the significance of soil supply to the process of debris flow formation via random disturbance of the normal hydrological process.

#### 1. Introduction

Debris flows, which occur frequently in mountainous catchments, are triggered by rainfall and are supplied with material from slope failures, landslides, rockfalls and fluvial sediment transport. As observed around the world, debris flows generally move in the form of surges (for example, Marchi et al., 2002; McCoy et al., 2012; Navratil et al., 2013; Hürlimann et al., 2014; Cui et al., 2018) that appear as a wave-like motion of high-density liquid with a certain volume and shape. As observed in Jiangjia Gully (JJG), a well-known debris flow catchment in southwestern China, each debris flow event comprises tens or hundreds of separate surges that have different discharges, densities and material contents. The findings of previous investigations of the spatiotemporal characteristics of surges within events (Wu and Kang, 1993; Li et al., 2003, 2004, 2008; Liu et al., 2008; 2009) suggest that surges should develop in a system with certain underlying dynamics that might include both deterministic and stochastic components (Hallerberg et al., 2007).

Many factors and mechanisms have been proposed that might operate to produce surge waves, such as the structure, fluid instability and

roll waves of debris flows (Weir, 1982; Ng and Mei, 1994; Wan and Wang, 1994; Hungr, 2000). Such theories originate from the perspective of flow movement and ignore the formation processes. However, observations indicate that successive surges have different properties; thus, as they are likely to originate from multiple sources, they cannot be described using a single flow model. As illustrated by processes on individual slopes (Guo et al., 2016a), intermittent and random failures might supply materials to debris flows in a process that leads naturally to separate surges. Thus, the formation mechanism of surges should be traced to the sources throughout a watershed.

Although monitoring on debris flow formation in headwater regions has been undertaken recently (for example, Marchi et al., 2002; McArdell et al., 2007; Hürlimann et al., 2014, 2019; McCoy et al., 2012; Navratil et al., 2013; Comiti et al., 2014; Cui et al., 2018; Theule et al., 2018; Coviello et al., 2019), and records of rainfall and related flows have helped reconstruct scenarios of debris flow occurrence, real-time formation processes have rarely been observed. This is understandable considering the risks and difficulties associated with obtaining field observations during an actual debris flow event.

Although debris flow discharge can be inferred from the rainfall and

<sup>\*</sup> Corresponding author at: No. 9, Section 4, Renminnan Road, Chengdu, 610041, China. E-mail address: aaronguo@imde.ac.cn (X. Guo).

X. Guo, et al. Journal of Hydrology 589 (2020) 125184

the material supplies, building such a reliable calculation method requires accurate and long-term monitoring of the involved parameters at an appropriate spatial scale and frequency. In practice, such monitoring typically encounters two great difficulties. First, rainfall has high spatial variability in mountainous valleys, which means that a single gauge cannot reflect local rainfall events, even within the confined region of a specific watershed (for example, Nikolopoulos et al., 2014, 2015; Guo et al., 2016b, 2016c; Cui et al., 2018). Second, a debris flow surge is a sudden event of short duration (usually lasting no longer than a few dozen seconds), which makes physical monitoring of such events problematic. Because of these difficulties, it can be hard to determine both the precise time of occurrence of a surge and the triggering rainfall, which hinders investigation of the process of debris flow formation. Fortunately, both long-term records of rainfall from widely distributed gauges and observations of debris flows in JJG have made it possible to trace the related hydrological processes and material supplies of debris flow events. The objective of the present study was to provide a comprehensive picture of surge formation based on 36 debris flow events, to illustrate how a surge develops as material sources respond to different rainfall amounts over an entire catchment.

#### 2. Study area and data source

#### 2.1. General introduction of JJG

Debris flow events occur frequently in JJG (approximately 10 events per year) and each event comprises tens or hundreds of separate surges, which makes the gully an ideal location for real-time monitoring of debris flows (for example, Davies, 1986, 1990; Li et al., 2003, 2004, 2008; Chen et al., 2005; Cui et al., 2005; Kang et al., 2006; Liu et al., 2008, 2009). Since its establishment in the 1960s, the Dongchuan Debris Flow Observation and Research Station, operated by the Chinese Academy of Science, has compiled a huge database of debris flows, which includes information on more than 500 events.

The watershed (Fig. 1) is located to the east of the Xiaojiang fault and is characterized by intense tectonics. The watershed is  $48.6~\rm km^2$ , and about 80% of the exposed rocks are highly fractured and mildly metamorphosed. Debris flows always occur in the rainy season (early June to late September) and the average annual rainfall ranges between  $400~\rm and~1000~\rm mm$ . The length of the mainstream channel is  $15.5~\rm km$ , and it comprises three sections: (1) the erosion zone (length:  $10.0~\rm km$ , average gradient:  $10.0~\rm km$ , average gradient: 10.

From the perspective of debris flows, JJG is a rather large valley. In such a watershed, a debris flow is not a full-valley process; rather, every surge originates only from certain tributaries depending on the spatial distribution and activity of potential source slopes. As the monitoring section is located near the station (Fig. 1), this study focused on the areas upstream of the section.

Currently, the principal material sources are distributed mainly in Menqian Gully (Fig. 1), where colluvium is distributed widely on the slopes and in the channels. There are three major tributaries in Menqian Gully, all of which have deep-cut channels with unstable slopes and broken rocks, and landslides in the source regions. Although the tributaries in the southern Duozhao Gully are also mantled with highly weathered rocks, check dams control the formation of debris flows.

#### 2.2. Data source

#### 2.2.1. Rainfall monitoring

Monitoring of rainfall in source areas is fundamental for predicting debris flow occurrence. For this purpose, 10 rain gauges have been installed in JJG, of which four (R1–R4) are located within or near the major source area (Menqian Gully; Fig. 1). These gauges measure rainfall using a 0.1-mm tipping bucket and the data are transmitted in

real time via the General Packet Radio Service.

Debris flow monitoring

In the following, the term "flow" includes both water flow and debris flow. Generally, "water flow" is difficult to monitor because of natural shifting of the riverbed and damage by frequent debris flows. Therefore, debris flows are the monitoring objective in JJG. For this study, debris flow parameters were measured manually and recorded at the monitoring section (Fig. 1). The appearance time of a debris flow front surge  $(T_1)$ , end time of the overall debris flow event at the monitoring section  $(T_2)$ , duration  $(D_f)$  and surge number (N) were recorded directly. The flow velocity (v) was determined using a stopwatch to measure the duration of the passage of the flow front through two sections within a 200-m-long channel (Fig. 2a), and flow height (h) and width (W) were estimated by experienced experts. The discharge (Q) was calculated using the expression Q = vh. Notably, this v is regarded as the velocity of the debris flow body, rather than the surface velocity. Additionally, samples of the moving debris flow bodies, which were collected using a volume-calibrated sampling container controlled by electronic devices (Fig. 2b), were used for density (p) and volume sediment concentration (CV) analyses.

#### 2.2.2. Data processing

This study considered data acquired from all 36 debris flows that occurred between 2006 and 2017 (Table 1). Information on one debris flow event as an illustration of the records of individual events is provided in Table 2. Each debris flow event comprised intermittent surges, continuative flows between the surges and the tail after the end of all surges. During the research period, the highest and lowest numbers of surges recorded in a single event were 98 and 3, respectively.

Each surge lasted approximately 10 s and the interval between surges ranged from tens to hundreds of seconds. The flows were typical high-density viscous debris flows with evident fronts and tails. The density of the surge flows was generally greater than 2.0 g/cm $^3$  with high concentration of fine particles. The discharge of the surges fluctuates by up to three orders of magnitude from < 10 to greater than 1000 (2262.5) m $^3$ /s.

Continuative flows generally occurred between two surges or persisted for longer than 0.5 h as a tail after the surges and their discharge was always  $< 10 \text{ m}^3/\text{s}$ . The density of the continuative flow was also as high as 1.7 g/cm<sup>3</sup> and even greater than 2.0 g/cm<sup>3</sup> in some cases.

#### 3. Activity of source material in the headwater regions

Field observations and photos shot by an unmanned aerial vehicle revealed that debris flows are potentially initiated by landslides, shallow slope failures, coalescing slope rills and erosion of loose slope—channel materials in tributaries. Here, Menqian Gully is taken as an example for introduction of source material activities (Fig. 3a).

Landslides are the main source type in the headwater region of the three tributaries. The mechanism via which rainfall infiltration can initiate shallow landslides is well known (Reid et al., 1988; Iverson et al., 1997, 2000). The landslides generally occur with heights of 30-200 m from the lowest channel to the top trailing edge on steep slopes of 35°-40° (Fig. 3b). Although not necessarily observed specifically, head erosion caused by landslides is known to be very active because farmland above the top edge of the landslides retreats markedly each year. In addition to the headwater region of the tributaries, landslides are also distributed densely along the channels in the upstream region of Menqian Gully (Fig. 3c). The gradients vary on the slopes above the channels (Fig. 3d). The upper sections with gradients of 20°-30° are covered with sparse shrubs and grass. Middle sections are covered by loose soils on slopes of 25°-30°. The shallow soils and steep gradients on the upper parts facilitate rainfall infiltration and surface runoff generation. The bedrock, which comprises mainly fragile Phyllite, is exposed on the lower sections with gradient of 35°-40°. The weathered rock surfaces are seriously eroded by upper runoff, and the

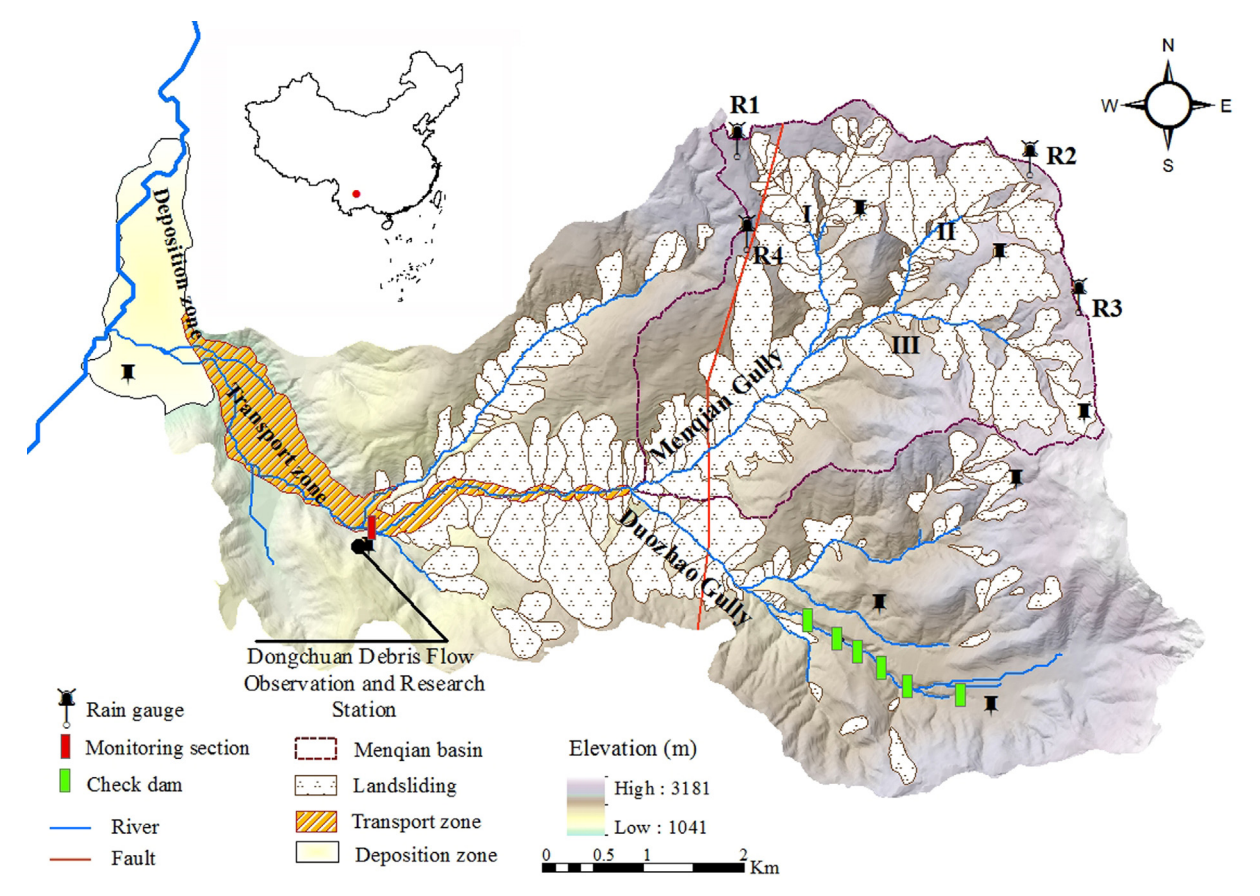


Fig. 1. Topographic map and location of monitoring stations in Jiangjia Gully.

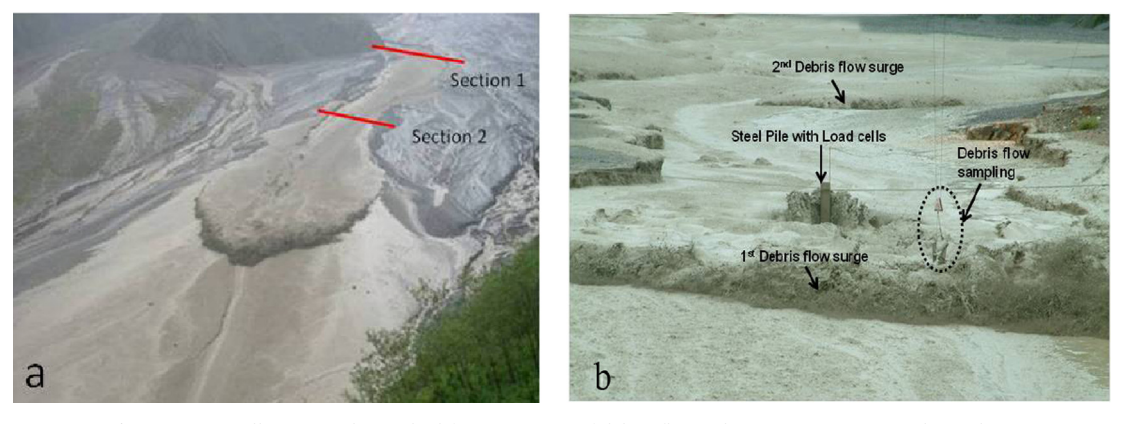


Fig. 2. Pictures illustrating the method for assessment of debris flow velocity measurement and sampling.

interflow stimulates translational landslides. The bottom of the slopes is generally loose colluvium with a natural angle of around 30°. Intense channel runoff during rainstorms also plays an important role through erosion of the slope colluvium, which increases slope instability and stimulates failure.

Along the channels, shallow slope residue and surface rill erosion frequently provide ubiquitous supply to the flow. The slopes, which are highly weathered and soil-mantled, are covered with deluvium (comprising gravels and clay particles) that is "ready" to fail under any circumstance (Fig. 3e). Slope rill formation is largely dependent on the local hydrological response of the various hillslope materials on the high steep slopes above the talus. The heads of the rills are largely exposed bedrock on steep slopes. As the slopes are naturally uneven in their lower part, the rills are formed by a combination of overland flow from relatively impermeable materials and lateral flow through highly

permeable materials. During periods of rainfall, intense precipitation in upstream areas causes a "firehose effect" by turning slope sediments into flow that deeply incises the channel and causes lateral erosion along the rills, which are predominately lined with fragile bedrock (Coe et al., 1997; 2008; Griffiths et al., 2004; Godt and Coe, 2007). The materials are deposited lower on the fans and downslope in the stream valleys. Although the material volume of each rill is relatively small, the dense distribution of the rills (for example, seven rills concentrated on a 200-m-wide slope) means that the fans combine to form a large deposit region in the channel (Fig. 3f).

The tributaries also act as crucial contributors to debris flow formation in the main channel. In the following, a right-hand small tributary with area of  $0.3~{\rm km}^2$  is taken for illustration. The upper region of the tributary is covered by sparse grass on a slope of  $20^\circ-25^\circ$ , which concentrates the overland flow during periods of rainfall. The debris

 Table 1

 Information on debris flow events monitored during 2006–2017.

No.	Date	$T_1$ (h:min)	$T_2$ (h:min)	$D_{\rm f}$ (h)	N	$Q_{\rm max}~({\rm m}^3/{\rm s})$	RG	$T_1/(h:min)$	τ (h)	DM	DT
1	2006-7-5	2:33	7:30	4.94	36	759.6	R1	0:15	0.4–1.6	II	b
2	2006-7-6	3:35	8:30	4.92	51	470.4	R1	2:16	0.5-1.3	II	b
3	2006-8-15	21:59	23:59	1.99	14	57.4	R1	17:46	0.7-1.2	I	a
4	2006-8-20	23:45	8:00	8.25	79	494.0	R3	18:46	0.8-1.6	II	b
5	2007-7-10	4:20	7:00	2.65	8	5.6	R2	23:37	0.8 - 2.2	I	a
6	2007-7-24	6:30	10:00	3.50	24	272.7	R1	0:00	1.7-2.0	II	c
7	2007-7-25	2:36	12:00	9.40	98	1358.3	R2	20:22	1.0-1.6	II	b
8	2007-7-25	14:24	18:30	4.10	62	2262.5	R1	10:56	0.3-0.7	II	b
9	2007-7-30	5:40	8:00	2.33	8	3.2	R2	1:55	1.0-1.4	I	a
10	2007-8-11	14:27	16:00	1.54	11	4.9	R3	11:40	1.0-1.3	I	a
11	2007-9-14	1:30	10:30	9.00	15	95.8	R1	19:44	0.65-0.85	I	a
12	2008-7-1	15:55	18:00	2.07	32	184.8	R4	4:25	0.6-1.6	I	a
13	2008-7-5	6:26	11:00	4.55	58	366.4	R2	3:39	0-0.8	II	b
14	2008-7-11	6:48	12:00	5.20	67	335.0	R4	6:18	0-0.5	II	b
15	2008-7-11	17:45	21:00	3.25	4	6.0	R4	17:08	0.3-0.5	I	a
16	2008-7-22	5:00	9:00	4.00	25	100.0	R3	22:55	0.2-0.5	I	a
17	2008-7-31	0:15	3:00	2.75	3	2.4	R1	20:58	0.2 - 2.5	II	a
18	2008-8-3	4:50	8:00	3.17	6	5.5	R1	0:11	0.3-0.8	I	a
19	2008-8-3	22:35	3:00	4.41	12	347.4	R2	16:48	2.0-2.7	II	c
20	2008-8-4	15:37	20:00	4.38	12	437.0	R1	10:04	0.5-1.0	II	b
21	2008-8-5	14:04	21:00	6.92	29	896.4	R4	13:29	0.3-0.6	II	b
22	2008-8-8	3:02	9:00	5.96	30	1118.4	R1	12:03	0.8-1.0	II	b
23	2008-8-11	2:33	5:00	2.44	9	118.3	R4	23:35	0.5-1.2	I	a
24	2008-8-17	19:00	22:00	3.00	3	4.1	R2	13:23	0.3 - 2.1	I	a
25	2009-8-4	5:24	9:00	3.60	41	194.8	R1	2:18	0.3-0.8	I	a
26	2010-7-6	5:23	9:00	3.62	12	59.3	R4	0:00	0-0.7	I	a
27	2010-7-17	20:39	1:00	4.34	55	256.5	R2	19:21	0-0.8	II	b
28	2010-7-22	19:15	23:00	3.74	30	82.6	R2	13:14	2.3-2.5	II	c
29	2010-7-24	19:00	21:00	2.00	5	8.5	R4	14:05	0.3-0.7	I	a
30	2010-8-5	5:51	9:00	3.14	5	1370.8	R3	18:48	10.3-10.9	II	c
31	2010-9-10	3:26	7:00	3.56	34	209.4	R4	1:39	0.7-1.6	I	b
32	2013-6-7	3:45	9:00	5.24	36	357.0	R3	1:37	0.8-2.1	II	b
33	2014-6-6	8:10	11:00	2.82	33	630.8	R3	0:56	2.8-7.2	II	c
34	2014-6-24	5:25	9:00	3.58	19	525.6	R1	22:51	2.7-6.1	II	c
35	2017-7-3	1:38	5:30	3.87	51	358.6	R4	22:09	0.3-1.3	II	b
36	2017-7-7	3:50	8:00	4.15	38	534.4	R2	1:11	1.6-2.2	II	c

 $T_1$ : debris flow appearance time at the monitoring section;  $T_2$ : debris flow ending time at the monitoring section (h:min);  $D_f$ : debris flow duration; N: surge number;  $Q_{\max}$ : maximum discharge; RG: rain gauge used in this work;  $T_1$ : rainfall start time;  $\tau$ : time lag of rainfall peak time and  $T_1$ ; DM: debris flow formation mode; DT: debris flow discharge type, I and II represent normal and abnormal types, respectively.  $T_1$ ,  $T_2$  and  $D_f$  are measured using stopwatch.

Table 2
Specific information of each surge of the debris flows in Jiangjia Gully (taking the 2007-7-24 event as an example).

Surge No	Flow type	Front time	Ending time	h (m)	W (m)	ν (m/s)	$Q (m^3/s)$	$\rho$ (g/cm <sup>3</sup> )	CV	Duration (s)
1	Intermittent surge flow	6:30:16	6:30:26	0.3	1.0	3.61	1.1	2.00	0.61	10
2	Intermittent surge flow	6:33:36	6:33:44	0.3	1.5	3.38	1.5	2.00	0.61	8
3	Intermittent surge flow	6:35:59	6:36:13	0.3	1.5	4.21	1.9	2.00	0.61	14
4	Intermittent surge flow	6:37:55	6:38:05	0.3	2.5	3.95	3.0	2.00	0.61	10
5	Intermittent surge flow	6:41:43	6:41:51	0.4	4.0	3.71	5.9	2.00	0.61	8
6	Intermittent surge flow	6:49:01	6:49:10	0.5	6.0	4.49	13.5	2.00	0.61	9
7	Intermittent surge flow	6:51:22	6:51:31	0.4	5.0	3.74	7.5	2.00	0.61	9
8	Intermittent surge flow	6:55:02	6:55:10	0.3	4.0	3.62	4.3	2.00	0.61	8
9	Intermittent surge flow	6:59:41	6:59:51	0.3	5.0	4.93	7.4	2.00	0.61	10
10	Intermittent surge flow	7:08:55	7:09:05	0.6	15.0	4.54	40.9	2.00	0.61	10
11	Intermittent surge flow	7:11:47	7:11:58	0.3	2.0	3.17	1.9	2.00	0.61	11
12	Intermittent surge flow	7:21:42	7:21:54	0.4	30.0	3.32	39.8	2.15	0.70	12
13	Intermittent surge flow	7:25:05	7:25:22	0.4	20.0	3.17	25.4	2.15	0.70	17
14	Intermittent surge flow	7:34:48	7:35:04	0.7	80.0	4.87	272.7	2.20	0.73	16
15	Intermittent surge flow	7:40:18	7:40:28	0.3	10.0	3.17	9.5	2.15	0.70	10
16	Intermittent surge flow	7:44:36	7:44:46	0.6	80.0	4.00	192.0	2.20	0.3	10
17	Intermittent surge flow	7:47:53	7:48:03	0.4	40.0	3.54	56.6	2.20	0.73	10
18	Intermittent surge flow	7:50:52	7:51:03	0.2	8.0	2.85	4.6	2.10	0.67	11
19	Intermittent surge flow	7:56:45	7:56:55	0.7	80.0	4.10	229.6	2.20	0.73	10
20	Intermittent surge flow	7:59:01	7:59:20	0.4	40.0	3.97	63.5	2.20	0.73	19
21	Continuous flow	8:07:06	8:30:00	0.3	3.0	3.00	2.7	2.00	0.61	1374
22	Continuous flow	8:30:00	9:00:00	0.2	1.5	2.50	0.8	1.93	0.56	1800
23	Continuous flow	9:00:00	9:30:00	0.2	1.0	2.00	0.4	1.80	0.49	1800
24	Continuous flow	9:30:00	10:00:00	0.2	1.0	1.80	0.4	1.75	0.46	1800

h: flow height; W: flow width; v: flow velocity; Q: flow discharge;  $\rho$ : flow density; CV: volumetric sediment concentration.

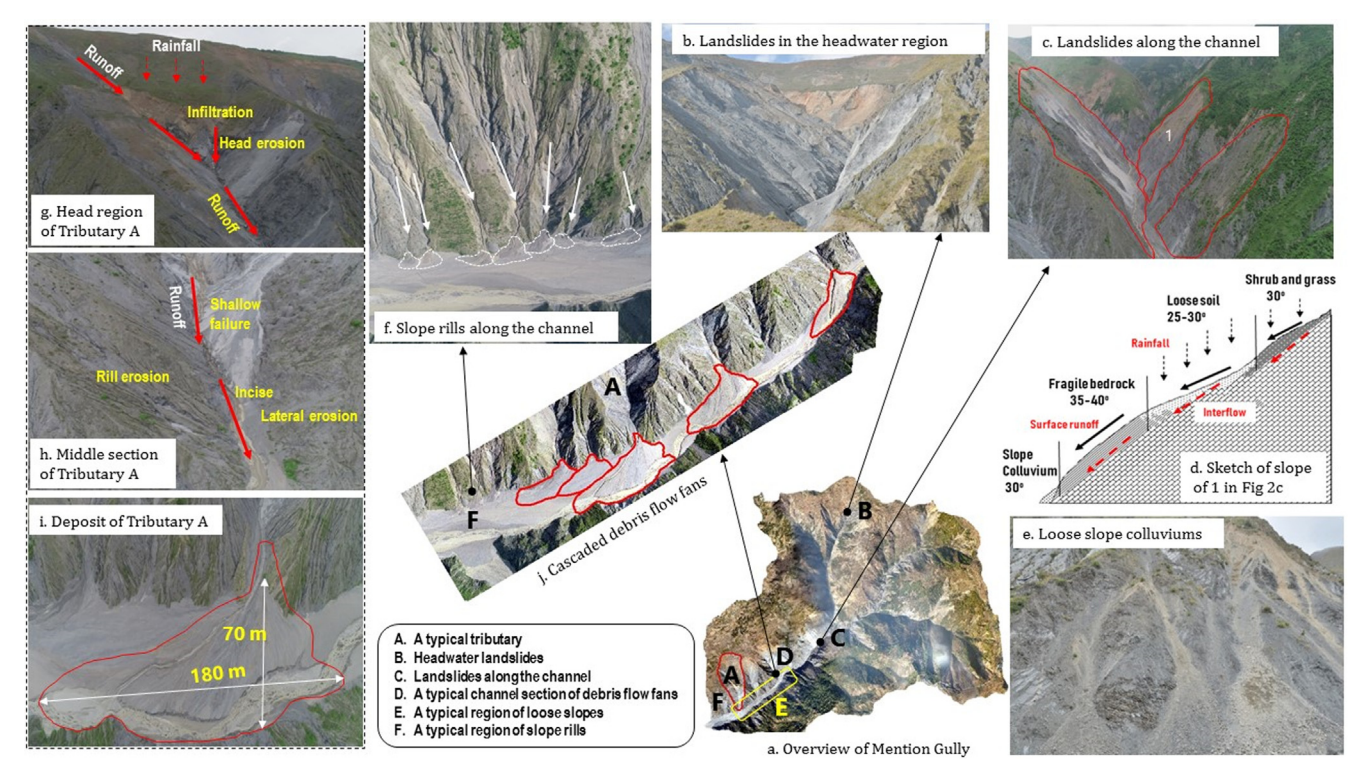


Fig. 3. Source materials and activities in Mengian Gully.

flow head region is a funnel-shaped trough, formed by head-erosionrelated landslide failure. The landslides are caused by the combination of rainfall infiltration and the lateral and incised erosion of upstream runoff (Fig. 3g). The channel is very steep and has a gradient similar to that of the slope, that is, 20°-25°. Along one side of the channel, small rills are densely developed on weak Phyllite bedrock outcrops; on the other side, loose weathered clastic particles accumulated widely on the slopes. These materials represent a nearly unending supply for debris flows. The severe deeply incised and lateral erosion significantly aggravate the aforementioned slope failures (Fig. 3h). The formed debris flow fan has length of about 70 m, which is sizable considering the relatively small area of the tributary. We inferred that debris flows historically blocked the channel, not only because the debris flow fan extends more than 100 m downstream in the main channel (Fig. 3i), but also because similar debris flow residues are evident on the other side of the river. The debris flow source supply and formation process are rather typical of tributaries in this region, that is, a steep slope, deep-cut channel, erodible slope surface and fragile exposed bedrock.

Although debris flows in the tributaries represent part of the flows formed in the main channel, the main processes differ because of the different controlling factors, such as channel slope conditions. In the tributaries, vertical and lateral erosion are intense; therefore, the debris flows formed move downstream quickly in response to the straight and steep channel conditions. Conversely, the channel-blocking phenomenon, which reduces the extent of vertical incision via changing the channel undulation, is evident in many sections in Menqian Gully. The formation of a landslide/debris flow dam relies on the material properties (such as volume, velocity and composition), runoff features (such as discharge, velocity) and interactive conditions (such as deflection/ confluence angle) (Dal Sasso et al., 2014; Fan et al., 2014; Chen et al., 2019). Nevertheless, in upstream areas, the considerable volume of the failure bodies, narrow channels (widths of only several meters) and direct interaction represent ideal conditions for instantaneous landslide blockages in the channel (Fig. 3c). Furthermore, in downstream areas, blockages of tributary debris flows are very obvious and serious, not only in terms of their spatial distribution, but also with respect to their

frequency of occurrence. For example, five cascaded debris flow fans were found in a 1.0-km channel section, several of which were closely connected (Fig. 3j); moreover, the vertical stratification of the fans showed that they were not formed by a single debris flow event. The failures processes of cascaded fan bodies are rather complex, which means it is difficult to determine their exact breaking time and magnitude (Cui et al., 2013).

Overall, the source materials of debris flows are distributed spatially throughout Menqian Gully, from the headwater region to the outlet (Fig. 1). We estimated that the debris flow source area is 9.4 km², accounting for around 73% of the entire area of Menqian Gully, which can be regarded as an unlimited supplier for producing debris flows. The abundant quantity of material and the diversity of supply modes result in a process of debris flow formation that is extremely sensitive to rainfall, in which the water requirement in the tributaries is reasonably low. It has been observed that debris flows can move at almost any time in small tributary channels, even with negligible water discharge, such as spring water.

#### 4. Hydrological process related to debris flows

#### 4.1. Identification of rainfall responsible for debris flows

As a debris flow forms from multiple sources in the tributaries and rainfall is distributed unevenly over the valley, it is difficult but fundamentally important to identify the rainfall responsible for debris flow occurrence. This involves determining where and at what time the flow begins. This can be achieved by comparing recorded surges and rainfalls and the spatial correlation between potential material sources and rainfall distribution.

The initiation time influences the determination of the rainfall event responsible for the flow (that is, the inducing rainfall amount and triggering intensity over 10 min, 30 min and 1 h), which ultimately influences the analysis of rainfall thresholds and flow formation processes. In fact, the initiation time is seldom known with precision; in most cases, the triggering time is assumed as the instant at which the

X. Guo, et al. Journal of Hydrology 589 (2020) 125184

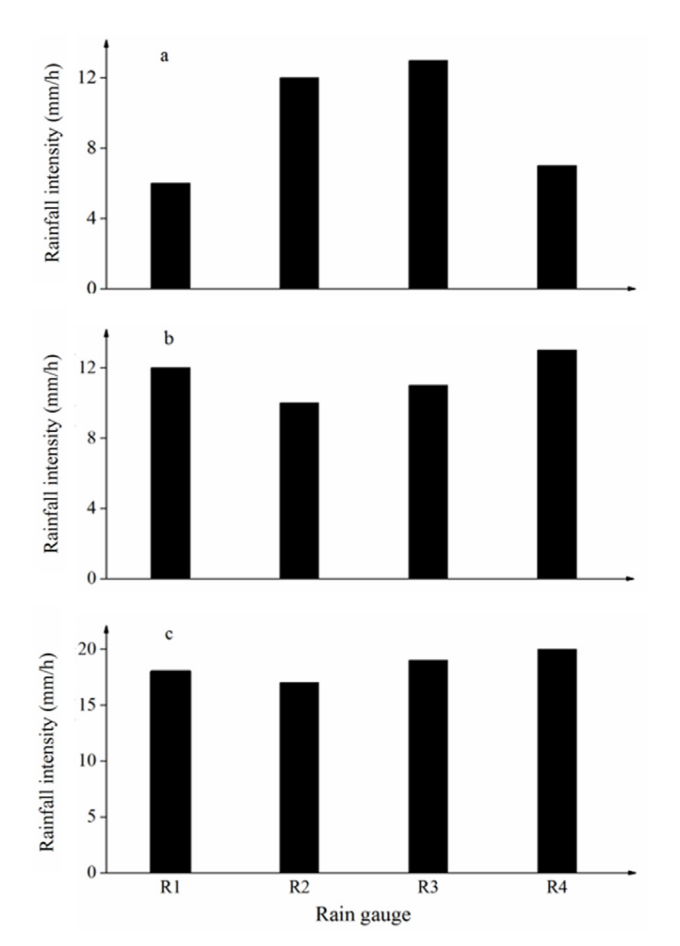


**Fig. 4.** Diagrams illustrating identification of rainfall responsible for debris flows (a. the areas neighboring R2 and R3 are regarded as the most likely potential source of debris flows; b. all slopes are considered potential source areas, and the arithmetic mean value was used; c. all slopes were considered the source regions, and the minimum value of the rain gauges were used.)

rainfall reaches maximum intensity (Iadanza et al., 2016). In this case, observations indicate that most occurrences (25/36) happened at rainfall intensities < 5 mm/h but with peaks in the tens of minutes prior to debris flow occurrence; thus, this peak period was taken as the rainfall period responsible for debris flow occurrence.

As rainfall is highly heterogeneous, even gauges R1–R4 in Menqian Gully, which are 2 km apart, present spatial variations; therefore, the rainfall recorded at the different gauges plays different roles in flow formation. Generally, the rainfall recorded at the four gauges presents the following features (Fig. 4).

- 1) Rainfall is very small (for example, < 5 mm/h) except for one or two gauges (for example, greater than 10 mm/h). The area(s) neighboring the exceptional rain gauge(s) could be regarded as the most likely potential debris flow source and thus the data from the gauge(s) were taken to represent the rainfall responsible.
- 2) Rainfall is uniform (for example, close to 10 mm/h). All slopes could be considered potential source areas and therefore the arithmetic mean value was used.
- 3) Rainfall recorded by all gauges was considerable (for example, > 15 mm/h). All slopes were considered the source region of debris flow initiation, but the minimum value of the rain gauges was used to attempt to identify thresholds.

Fig. 4. Diagrams illustrating identification of rainfall responsible for debris flows

Using this determination method, the gauges used for a debris flow were identified as listed in Table 1 (RG). It must be admitted that this identification is not a systematic procedure but relies on experience and

on knowledge of debris flow formation processes. However, this is unavoidable, and the error could be controlled to a certain extent through consideration of the universal regulation derived from using more than 30 events that provided actual rainfall cases with spatial differences. The key point is that both the rainfall amount threshold for debris flow initiation and the time lag from peak rainfall to debris flow appearance (discussed in the following) can be quantified based on this temporal and spatial identification procedure.

Based on determination of the location and initiation time of a debris flow, the characteristics of the rainfall event can be estimated from the available rain gauge data. The following indices are of special interest.

- 1) Inducing rainfall (*R*<sub>I</sub>, mm): the cumulative rainfall from the beginning of the rainfall event to the time of debris flow occurrence.
- 2) Mean inducing rainfall intensity (*I*, mm/h): obtained by dividing the inducing rainfall (*R*<sub>1</sub>) by the duration from the beginning of the rainfall event to the time of debris flow occurrence (*D*).
- 3) Triggering rainfall ( $R_T$ , mm): the direct triggering rainfall in 1-h, 30-min and 10-min periods.
- 4) Antecedent rainfall (R<sub>a</sub>, mm): the weighted sum of rainfall days prior to the occurrence of a debris flow, which can be defined as (Cui et al., 2007; Guo et al., 2013, 2017):

$$R_a = \sum_{i=1}^{n} R_i(K)^i$$
 (1)

where  $R_i$  is the daily rainfall in the preceding n days, i designates the exact number of days prior to the debris flow incident  $(1 \le i \le n)$ , and K is a decay coefficient of the i-th day. Suggested values for K and n are 0.8 and 10, respectively.

Statistical information of the rainfall is listed in Table 3. Among other factors, inducing rainfall ( $R_{\rm I}$ ) and triggering rainfall ( $R_{\rm T}$ ) are the direct causes of debris flow occurrence (Guo et al., 2016c, 2017). It is evident that the value of each rainfall factor varies markedly; for example, the inducing rainfall amount varies from 5.1 to 58.4 mm, and the triggering 10-min, 30-min and 1-h rainfall varies in the ranges 1.1–15.3, 3.0–27.4 and 5.1–50.8 mm, respectively. This indicates the difficulty of predicting debris flows based on a single parameter and reveals that the triggering condition is highly uncertain. Therefore, the reasons for debris flow occurrence should be investigated comprehensively.

#### 4.2. Hydrological calculation for water flow estimation

On the watershed scale, a debris flow is considered a product of a rainfall induced hydrological process involving the supply of soil material. This involvement influences the flow discharge, density and time of peak discharge. From a hydrological perspective, the discharge and time lag from peak rainfall to debris flow appearance at the monitoring section appear to take special roles in reflecting the runoff yield and flow influx processes. Notably, shallow soil failures and rill erosions contribute primarily to frequent "normal" debris flows, whereas a landslide/debris flow dam-outburst usually results in a catastrophic ("abnormal") debris flow, according to the classification of Bardou and Jaboyedoff (2008). A normal hydrological process is water-dominated and the debris flow hydrograph comprises water and instantaneous sediment volume. In an abnormal debris flow, the time lag might be longer than normal and the peak discharge would be amplified considerably because of the blockage outburst, as observed in many other sites (Cui et al., 2013; Zhou et al., 2013, 2015).

In this watershed, a combined rainfall–runoff and routing method was used to estimate the maximum water flow because data on water flood discharges are unavailable. This method has also been applied in related previous research (Lumbroso and Gaume, 2012; Capra et al., 2018). First, the rainfall was interpolated using the Thiessen polygon

Journal of Hydrology 589 (2020) 125184

 Table 3

 Rainfall conditions responsible for debris flow occurrence.

Date	N	$Q_{\rm max}~({\rm m}^3/{\rm s})$	$R_{\rm I}$ (mm)	RG	D (h)	I (mm/h)	$R_a$ (mm)	$R_{\text{max-1h}}$ (mm)	$R_{\text{max-30 min}}$ (mm)	$R_{\text{max-10 min}}$ (mm)
2006/7/5	36	759.6	25.1	R1	2.25	11.2	15.3	14.5	8.8	5
2006/7/6	51	470.4	18.9	R1	0.67	28.2	32.6	18.9	12.8	6.2
2006/8/15	14	57.4	30.6	R1	5.5	5.6	19.6	27.9	27.4	14.7
2006/8/20	79	494	10	R3	6.5	1.5	8.6	5.3	5.3	3.4
2007/7/10	8	5.6	29	R2	8.5	3.4	13.5	13.2	7.7	5.3
2007/7/24	24	272.7	18.3	R1	6	3.1	25.2	7.9	4	1.7
2007/7/25	98	1358.3	33.8	R2	5.67	6	23.5	15.3	10.6	5.3
2007/7/25	62	2262.5	58.3	R1	4	14.6	33.3	11.6	10.5	4.8
2007/7/30	8	3.2	21.5	R2	3.4	6.3	33.2	14.1	6.6	4.5
2007/8/11	11	4.9	15.8	R3	2.67	5.9	5.1	13.4	8.2	4.4
2007/9/14	15	95.8	18.2	R1	5.25	3.5	18.1	11.7	6	3.8
2008/7/1	32	184.8	24.1	R4	10	2.4	10.8	15.2	8.5	6.5
2008/7/5	58	366.4	14.1	R2	2.33	6.1	16.6	14.1	12.1	5.6
2008/7/11	4	6	5.1	R4	0.5	10.2	14.2	5.1	5.1	4.1
2008/7/11	67	335	17.7	R4	0.5	35.4	9.8	17.7	17.7	11.7
2008/7/22	25	100	25.6	R3	5.5	4.7	13.5	12.8	11.2	9.4
2008/7/31	3	2.4	29.1	R1	3	9.7	10.8	18.9	17.3	12.4
2008/8/3	6	5.5	18.6	R1	4.3	4.3	21.6	14.9	8.8	4.3
2008/8/3	12	347.4	28.6	R2	5.2	5.5	40.2	26.4	22.4	8.7
2008/8/4	12	437	11.3	R1	3.5	3.2	21.6	10.6	10.3	6.4
2008/8/5	29	896.4	9.4	R4	0.5	18.8	61.3	9.4	9.4	4.7
2008/8/8	30	1118.4	30.9	R1	14.5	2.1	40	5.6	3	1.1
2008/8/11	9	118.3	8.3	R4	2.4	3.5	37.5	7.1	4.8	3
2008/8/17	3	4.1	13	R2	4.8	2.7	18.2	6.5	5	2
2009/8/4	41	194.8	31	R1	2.7	11.5	53.4	24.6	19.6	11
2010/7/6	12	59.3	21.5	R4	5	4.3	10.8	18.4	15.4	9.6
2010/7/17	55	256.5	18.8	R2	1	18.8	8.1	19	15.6	11.9
2010/7/22	30	82.6	12.3	R2	3.7	3.3	13.5	11.3	11.3	10.6
2010/7/24	5	8.5	9.7	R4	3.1	3.1	25.2	9.3	9.3	8.1
2010/8/5	5	1370.8	25.8	R3	1.9	13.6	29	24.4	22.7	15.3
2010/9/10	34	209.4	42.4	R4	1	32.6	10.8	41.9	13.4	6
2013/6/7	36	357	58.4	R3	1.7	34.4	13	50.8	15.4	7.7
2014/6/6	33	630.8	36.1	R3	8.2	4.4	17.8	10.1	5.3	3.4
2014/6/24	19	525.6	25	R1	6	4.2	26.6	7.1	5.5	3.8
2017/7/3	51	358.6	35.2	R4	3	11.7	42	24.8	18.4	8.1
2017/7/7	38	534.4	31.1	R2	2.2	14.1	37.7	28.1	17.7	9.2

N: surge number;  $Q_{\max}$ : maximum discharge;  $R_1$ : inducing rainfall for debris flows; RG: rain gauge employed; D: rainfall duration from start of rainfall to debris flow occurrence; I: mean rainfall intensity in period D;  $R_a$ : antecedent rainfall;  $I_{\max-1h}$ : maximum rainfall amount in 1 h;  $I_{\max-30 \text{ min}}$ : maximum rainfall amount in 30 min;  $I_{\max-10 \text{ min}}$ : maximum rainfall amount in 10 min.

method and the watershed was divided into subregions based on units of slope. Then, for each slope subregion, the runoff yield was calculated based on the US Soil Conservation Service (SCS) Curve Number (CN) method (SCS, 1985; Mishra and Singh, 2003). In the SCS method, the volume of water runoff produced is estimated through the single parameter CN, which summarizes the influence of both superficial aspects and deep soil features including the saturated hydraulic conductivity, type of land use and humidity before the precipitation event. We suggest that the larger the value, the greater the runoff yield. Generally, CN values are identified via a lookup table from the handbook (SCS, 1985). The kinematic wave routine method was used to simulate the propagation and influx process of the water flow.

#### 4.3. Validation of the hydrological calculation

Validation of the results for water flow was rather difficult because of the lack of measurements of water flood discharges. In recent studies, validation was performed by comparing the time of the peak of the simulated hydrograph with the time of detection of debris flow occurrence at monitoring stations at other sites (Lumbroso and Gaume, 2012; Capra et al., 2018). In this work, the validation process not only compared the time lag  $\tau$ , also compared the total water flow amount.

Time lag

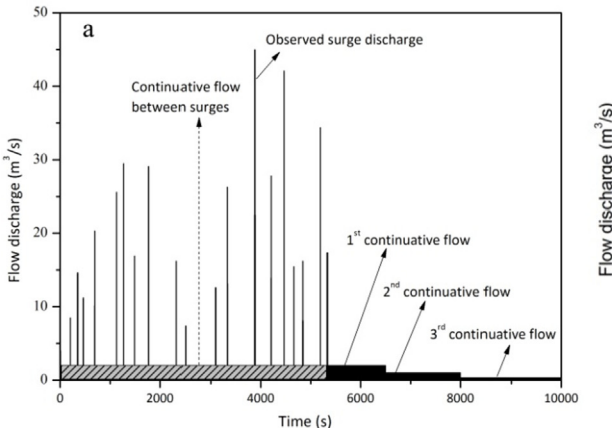
The time lag  $(\tau)$  from the time of the triggering rainfall to debris flow appearance at the monitoring section is a principal index that represents the propagation process. After identification of the rainfall responsible for a debris flow, the time lag  $(\tau)$  can be analyzed through

comparison of the rainfall and surge hydrograph. The results indicate that time lag  $\tau$  generally falls within the range of 30 min to 1.1 h (average: 50 min, Table 1), depending on the material supply and flow influx processes.

This lag is therefore considered a key parameter for distinguishing normal and abnormal events. For normal cases, we inferred that the peak rainfall period is within 1 h of debris flow appearance. However, in some abnormal cases, the lag is much longer, as listed in Table 1. For example, the 2010–8-5 debris flow captured at the monitoring section at 05:51 (all times given are local time) occurred 10.5 h after the peak rainfall and even 10 h after the rain stopped, which indicates that the debris flow was not an instant response to the rainfall. The hydrological simulation is unsuitable under such circumstances. Therefore, the simulation and validation of water flow were performed only for events with a normal time lag (that is,  $\leq 1$ h).

Total water flow volume

Because the debris flow surges rather than the real water flow hydrographs were measured directly, the calculation of the total water amount should be explained. As shown in the generalized sketch (Fig. 5a), a monitored debris flow hydrograph comprises several discontinuous surges together with continuative flows between the surges, and continuative flows appear as tails after the surges have ended. For continuative flows between two surges that were not completely recorded, we assumed that they had discharge  $Q_d$  and CV values similar to those of the first continuative flow after all surges had ended. The total volume of a surge is simplified as a triangle-shape because the discharges of the debris flow front and tail are different, whereas a



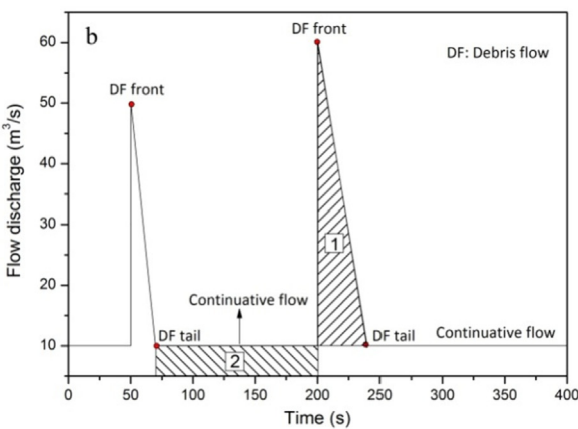


Fig. 5. Generalized sketch of the water flow discharge calculation.

continuative flow is relatively steady and can be simplified as a rectangle-shape for volume calculation. As a debris flow is a mixture of water and soil, the water flow discharge  $(Q_w)$  of each surge can be estimated based on the debris flow discharge  $(Q_d)$  using Eq. (2):

$$Q_w = Q_d(1 - CV) \tag{2}$$

and the total amount is the integral sum of the surges and the following continuative flows.

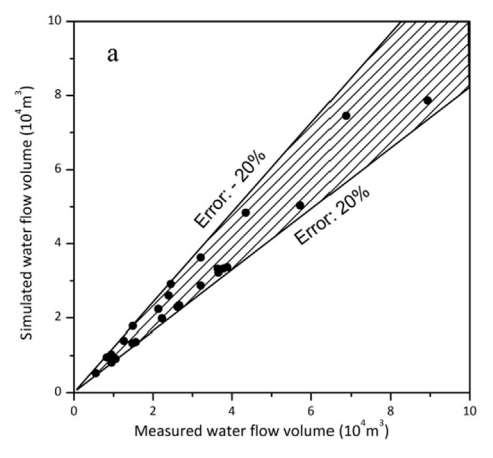
Considering both the uncertainty in monitoring and the assumptions in the data processing of the total water flow amount, an acceptable error range of [-20%, 20%] was adopted. As shown in Fig. 6a, the simulation errors are in the range of [-15.6%, 17.7%] with an average value of 7.2%. The Nash–Sutcliffe efficiency coefficient is 93% and the correlation coefficient is 96%. Meanwhile, the debris flow occurrence time corresponds to the peak water discharge period (Fig. 6b). The validation of flow propagation time and total flow amount verified the parameters used in the hydrological calculation, which allowed the simulation's acceptable accuracy and provided a method with which to assess any obvious abnormal relation between water flow discharge and debris flow discharge.

#### 4.4. Criterion for discriminating normal from abnormal events

The real ratio of debris flow discharge to water flow discharge is generally under the upper limit value of 3.3, considering that the measured CV is in the range 0.514–0.767. However, the conditions of the ratio (Y) between the debris flow discharges and calculated water flow discharges differed. This can help to distinguish normal from abnormal events. For instance, the 2013–6-7 event was used as a case

study to illustrate this ratio (Fig. 7). It was selected because it had the highest event rainfall (77.0 mm) and 1-h rainfall intensity (50.8 mm/h) of all the studied events (as recorded at R2). Moreover, it also had considerable antecedent rainfall of 34.4 mm during the 10-d period prior to the event date. The actual value used to represent the real runoff yield condition for peak discharge was approximately 90 m<sup>3</sup>/s. The simulated peak flow time was 03:30-04:00 and the first debris flow surge was monitored at 03:45. Additionally, we also used for reference a value of CN = 90 for the entire watershed, which is very high and almost impossible to achieve, especially for the high permeability of the loose material of the soil surface in the source region. The result indicates that the upper limit of runoff discharge in this watershed (Fig. 7) was no greater than 120 m<sup>3</sup>/s. In this case, the potential maximum value of debris flow discharge is in the range of 360–480 m<sup>3</sup>/ s, based on Eq. (2). The ratio  $\gamma$  is regarded as normal because the monitored debris flow discharge was 357 m<sup>3</sup>/s.

In some cases, the upper limit of the simulated water flow peak discharge was much smaller than the monitored debris flow discharges. For instance, the simulated maximum  $Q_{\rm w}$  of the 2007–7-25 event was 53.8 m³/s and the monitored CV at the simulated peak water flood period was in the range of 0.72–0.75, which indicates that the debris flow discharge  $Q_{\rm d}$  was in the range of 192.1–215.2 m³/s. Additionally, the potential maximum water flow (CN=90) was 66.4 m³/s, which indicates a debris flow discharge  $Q_{\rm d}$  with an upper limit of 265.6 m³/s. However, the monitored peak discharge of  $Q_{\rm max}=2263$  m³/s is much higher than this value. In this circumstance, the relation is considered abnormal because it does not reflect a normal hydrological process; instead, it represents the outburst of blockage bodies in the upper steam, which significantly amplify the discharge.



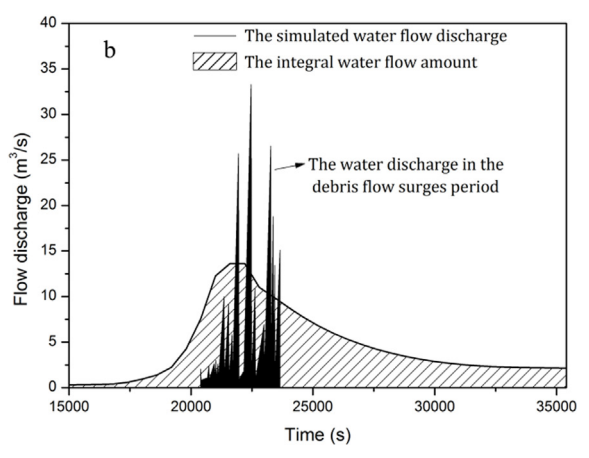


Fig. 6. Simulation result of the hydrological model: (a) validation with the total water amount and (b) hydrograph of one case 2008-7-11 for illustration.

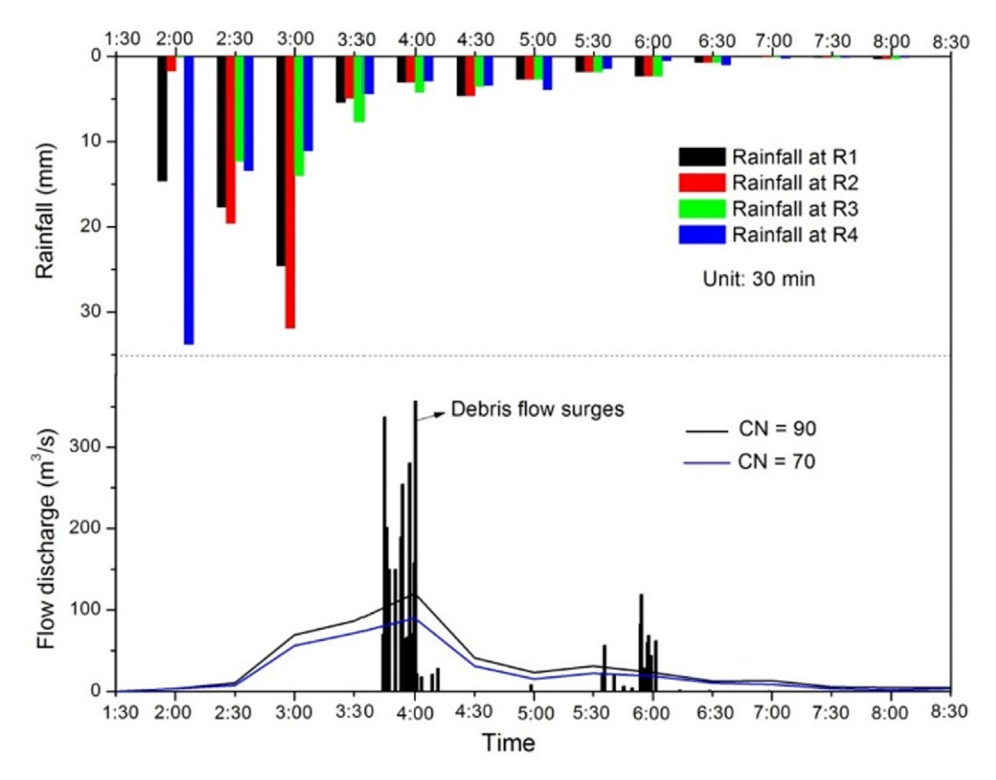


Fig. 7. Calculated water flood discharge of the 2013-6-7 rainfall event.

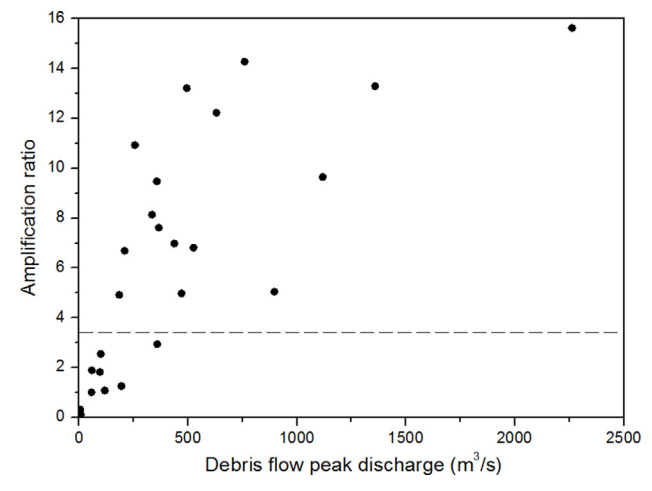


Fig. 8. The ratio between the debris flow discharge and water flow discharge.

The ratio  $\varUpsilon$  of more than 50% of debris flows was greater than 3.3 (Fig. 8). The maximum  $\varUpsilon$  was 15.6, which indicates a significant amplification effect.

#### 5. Possible processes of debris flow formation

In this section, the hydrographs of some typical debris flow cases are taken as examples with which to explain the hypothesis and the rainfall conditions required are analyzed to indicate the formation processes.

#### 5.1. Typical cases analysis

#### 5.1.1. Events with normal $\tau$ and $\Upsilon$

As shown in Fig. 9, the rainfall in the 2009–8-4 event was concentrated between 04:30 and 05:45 and the debris flow appeared at the monitoring section at 05:24. At the beginning of the event, the rainfall peak started at R1 with a peak amount of 13.3 mm in 15 min

(04:32-04:46). This was followed shortly by a burst of rainfall at R4 (04:38-04:57) with a peak amount of 18.3 mm. Although the rainfall recorded at R3 was smaller than at R1 and R4, the peak lasted longer—until 05:05—with 18.5 mm recorded in the previous 30 min. The rainfall values recorded were all sufficient to induce debris flows according to historical records (Guo et al., 2013). Therefore, it is difficult to identify the exact time and location of the debris flow initiated during 04:30-05:00. However, by comparing the rainfall and debris flow processes, the time lag was identified as 36-54 min. The rainfall continued over the gully; therefore, all the tributaries might have been activated to supply materials. Even within the short peak period of 30 min, the alternate peaks in the different tributaries might have expanded the region of debris flow initiation and extended the period of slope failure, which potentially increased the number of surges and the duration of the debris flow. The mean discharge of this debris flow was 60.6 m<sup>3</sup>/s with a peak of 194.8 m<sup>3</sup>/s. The debris flow surges persisted until 06:18. Although the flow after this time was still a type of debris flow, it was more representative of a tail that behaved as a continuative flow with a much smaller discharge.

The hydrological simulation shows that the peak period of water flow discharge concurred with debris flow occurrence, with a peak value of 64.3 m $^3$ /s. The ratio  $\Upsilon$  was in the range of 1–3, which is reasonable for a normal water–soil mixture. The debris flow formation processes in the source region were not observed in situ; however, it can be inferred that slope failures occurred continuously in all tributaries and that the material became intermittently mixed with the water flood.

#### 5.1.2. Events with a normal $\tau$ and abnormal $\Upsilon$

The 2008–8-8 debris flow event (Fig. 10) accompanied rainfall of long duration (32 h) and low intensity (< 6 mm/h) at each rain gauge. However, it followed a considerable amount of antecedent rainfall (40.0 mm according to R4) that fell on August 5–7. The debris flow was monitored at 03:02 on July 9, approximately 14.5 h after the rainfall began, and the front discharge was 73.4 m<sup>3</sup>/s. Eight surges were captured during 03:02–03:38, that is, one surge approximately every

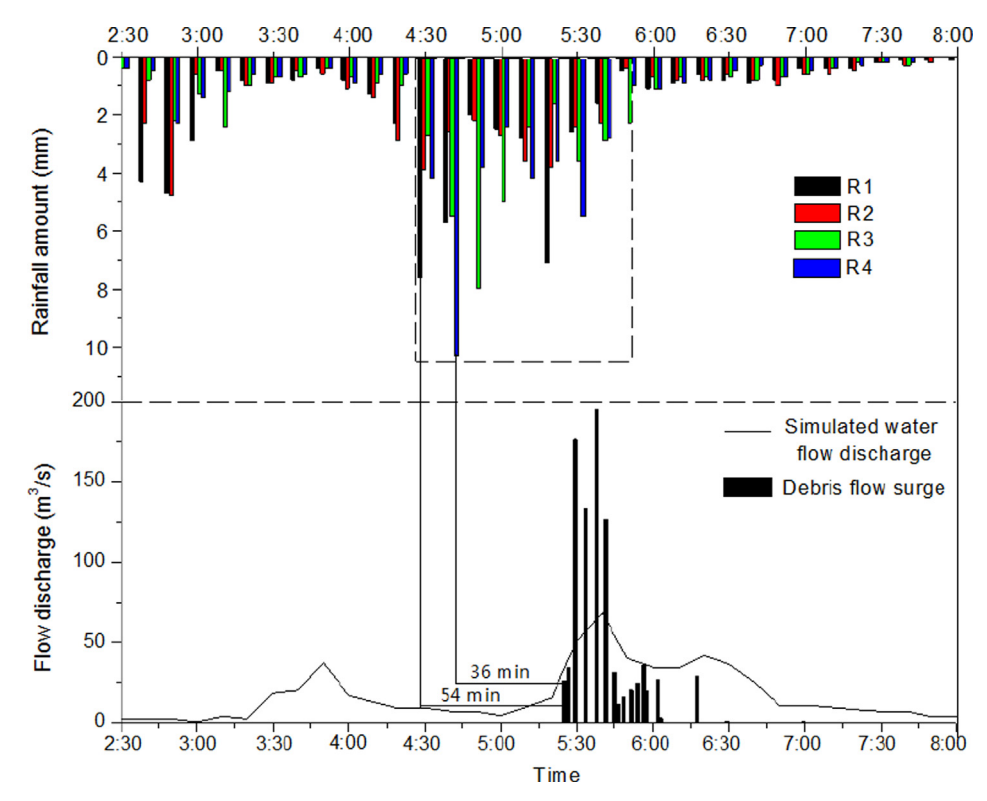


Fig. 9. Rainfall and debris flow processes on 2009-8-4.

4.5 min. Seven minutes later—at 03:45—the ninth surge discharge was monitored to be 632.9  $\rm m^3/s$ . This was followed by the 10th surge, which had a discharge of 110.8  $\rm m^3/s$ , at 03:46. The 11th–13th surges, which had discharges of 515.5, 41.0 and 1118.4  $\rm m^3/s$ , occurred at 03:55, 04:07 and 04:26, respectively. Subsequently, there were two

further large discharges, which lasted over 10 min and had discharges of 445.6 and 534.5  $\ensuremath{m^3/s}.$ 

This event did not represent a normal hydrological process because the debris flow discharges (up to 1118.4  $\rm m^3/s)$  were much higher than the upper limit estimates (no more than 120  $\rm m^3/s$  in this case), which

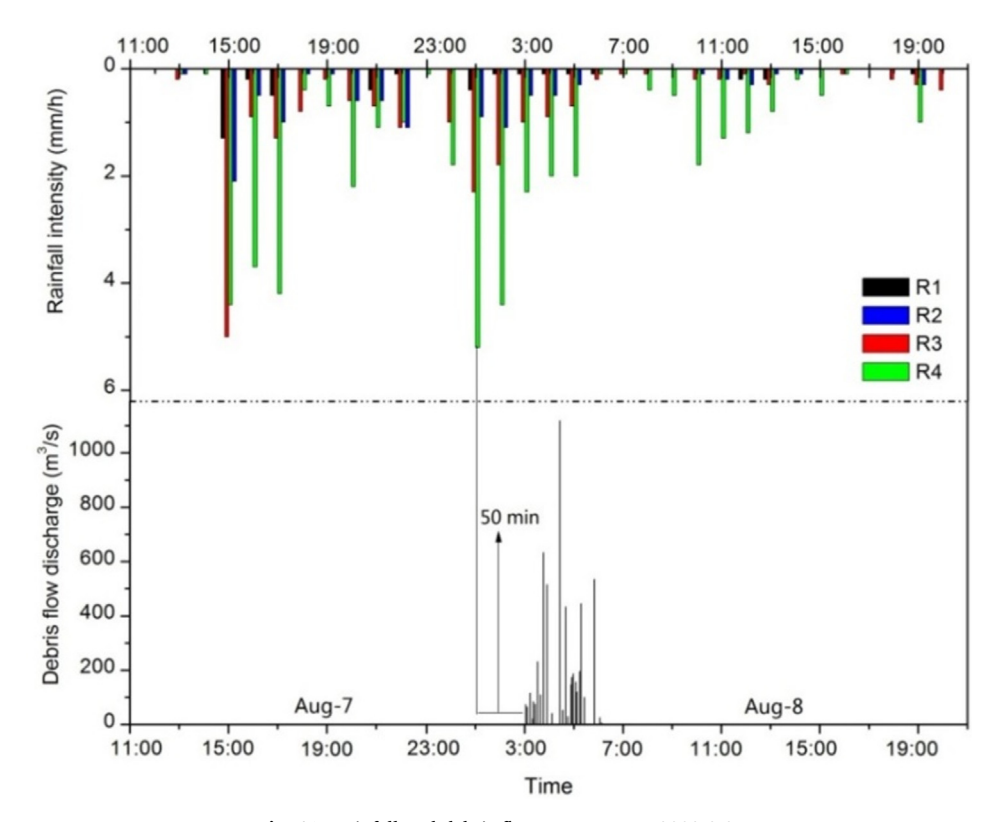


Fig. 10. Rainfall and debris flow processes on 2008-8-8.

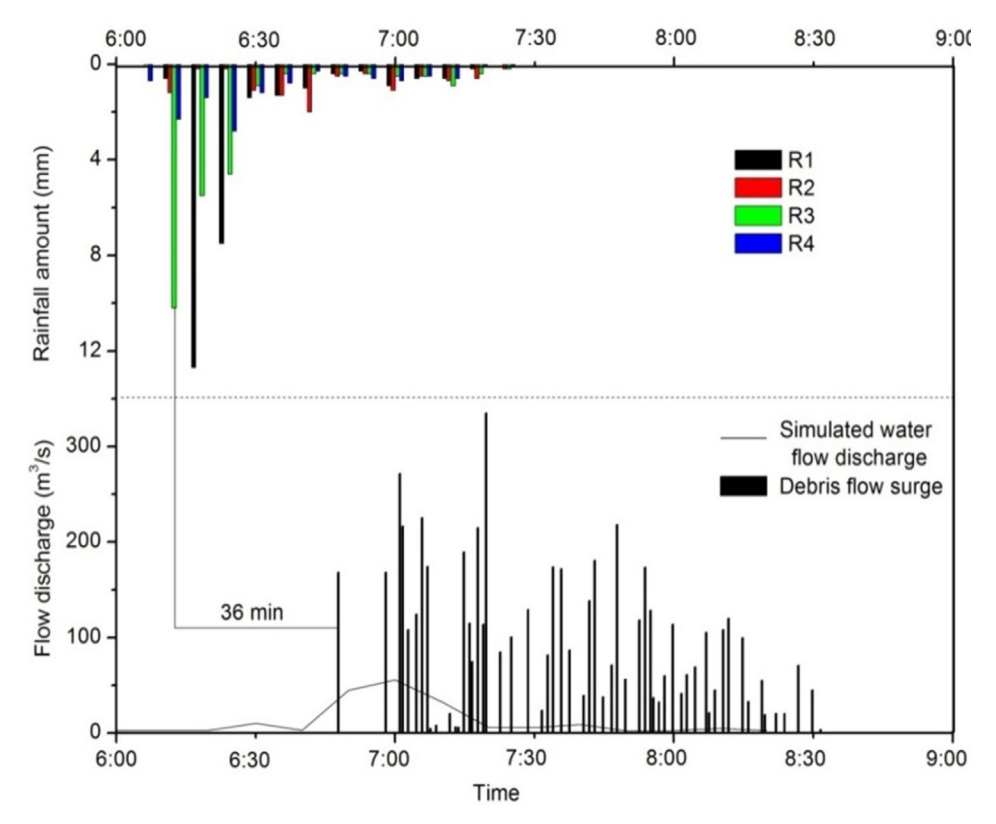


Fig. 11. Rainfall and debris flow process on 2008-7-11 (debris flow appeared as a continuative tail flow with small discharge of 0.5 m<sup>3</sup>/s from 08:30–11:00).

indicates the occurrence of a blockage–breaking effect in the source regions, although it was not monitored in situ. It seems that there was a time lag for runoff accumulation, and that this time generally exceeded 7 min and up to 24 min, which suggests that failures of either landslides or tributary debris flows blocked the channels before such accumulation. In this case, the failures did not require high-intensity rainfall because of the abundant antecedent rainfall condition. Assuming fresh blockage bodies are sufficiently loose and prone to failure, the accumulation time depends on the runoff discharge and the hydraulic infiltration process in the dam body. Such failures and blockage bodies in the source regions could occur intermittently several times. This process controls debris flow formation, which explains the appearance of the surges.

Another case with a similar discharge profile was the 2008–7-11 event (Fig. 11), although this occurred following a short period of intense rainfall. The rainfall was concentrated from 06:22–06:50 on July 11. The rainfall at R1 and R3 (20.8 and 20.5 mm, respectively) during the 0.5-h period before the debris flow was much higher than at R2 and R4, which indicates that the slopes of tributaries I and III were more likely to become source areas. The first debris flow surge was monitored at 06:58 with discharge of 168.1 m³/s. The second surge followed 3 min later with discharge of 271.8 m³/s. Subsequently, further surges with discharge greater than  $100 \text{ m}^3$ /s appeared intermittently at intervals of 1 to several minutes, and the peak discharge of 335.0 m³/s was monitored at 07:20. The intermittent surges persisted until 08:30, following which continuative flow as a tail lasted until 11:00.

The recorded data show that the rainfall amount was small after 06:30, although the rainfall continued until 07:20. This is interesting because debris flow surges with high discharge continued to appear after this time. This suggests that channel runoff but not rainfall was the causative factor of this debris flow. Therefore, in this case, the intense rainfall during 06:22–06:50 caused the failures that formed the initial debris flow, as confirmed by both the observed time lag of approximately 30 min and the hydrological calculation results. The calculated peak water discharge was 55.2 m<sup>3</sup>/s, which indicates a reasonable soil

concentration rate. However, given that the ratio  $\Upsilon$  was much larger than 3.3 for most of the time, repeated dam failures could have been the principal reason for the subsequent surges. The maximum peak discharge and numerous large discharges of greater than 200 m<sup>3</sup>/s, together with the long duration of the debris flow after the end of the rainfall peak, support this inference.

#### 5.1.3. Events with abnormal $\tau$ and $\Upsilon$

In the 2010-8-5 event (Fig. 12), the rainfall was concentrated during 18:48-20:41 on August 4, and the rainfall recorded at R1 and R2 (18.9 and 25.3 mm, respectively) was much higher than at the other two gauges (12.7 and 7.3 mm), which suggests that the areas with greatest potential for slope failure were in tributaries I and II. The debris flow was monitored at 05:50 on August 5; its discharge was 1370 m<sup>3</sup>/s. The time lag of almost 10 h was much longer than normal and the discharge was much higher than a normal water flood. This suggests that failures that might have occurred during or after the rainfall event did not form debris flows immediately but instead blocked the channels. This blocking was not realized at the monitoring section because water flows originated normally from the other tributaries in JJG. However, the blockage body eventually outburst and formed a huge debris flow at 05:50 on August 5. The sole intermittent surge and the following continuative flow suggest that the entire body burst in one instant. The rainfall during the period 18:48-20:41 in tributaries I and II induced blocking dam formation via landslides in the upper stream/tributaries, and the constant upstream flow after the end of the rainfall was the direct trigger of dam breaking and debris flow formation in the main channel.

#### 5.1.4. Multiple debris flows in one long-duration rainfall event

Sometimes multiple debris flows occur during a single rainfall event, which highlights the diversity of debris flow formation types in this watershed. These events are actually combinations of the three types described above; for instance, the rainfall event of July 23–25, 2007 (Fig. 13) triggered three debris flow events that comprised 24, 98

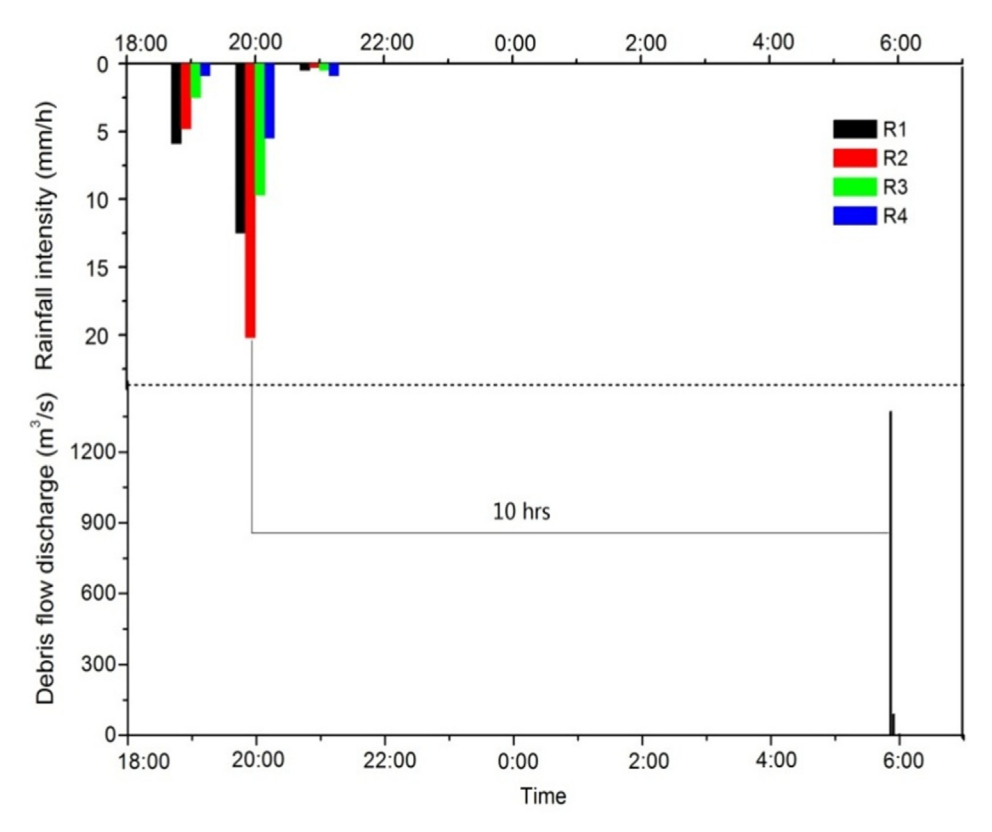


Fig. 12. Rainfall and debris flow process on 2010-8-5.

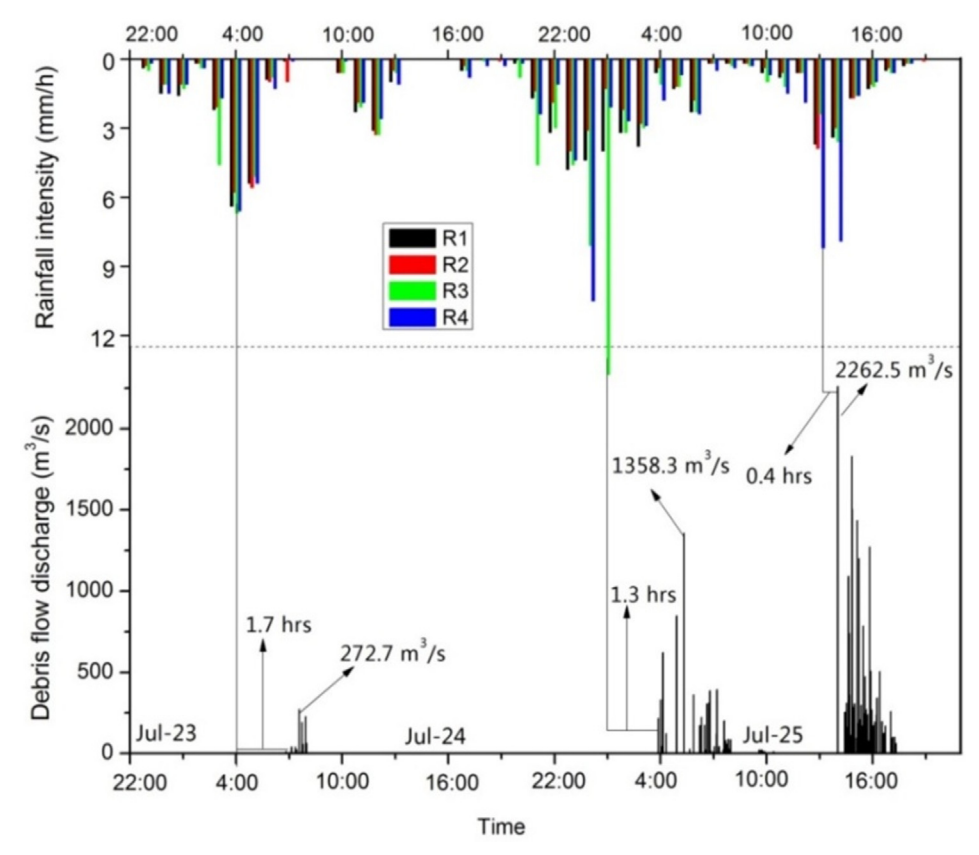


Fig. 13. Rainfall and debris flow processes on July 23-25, 2007.

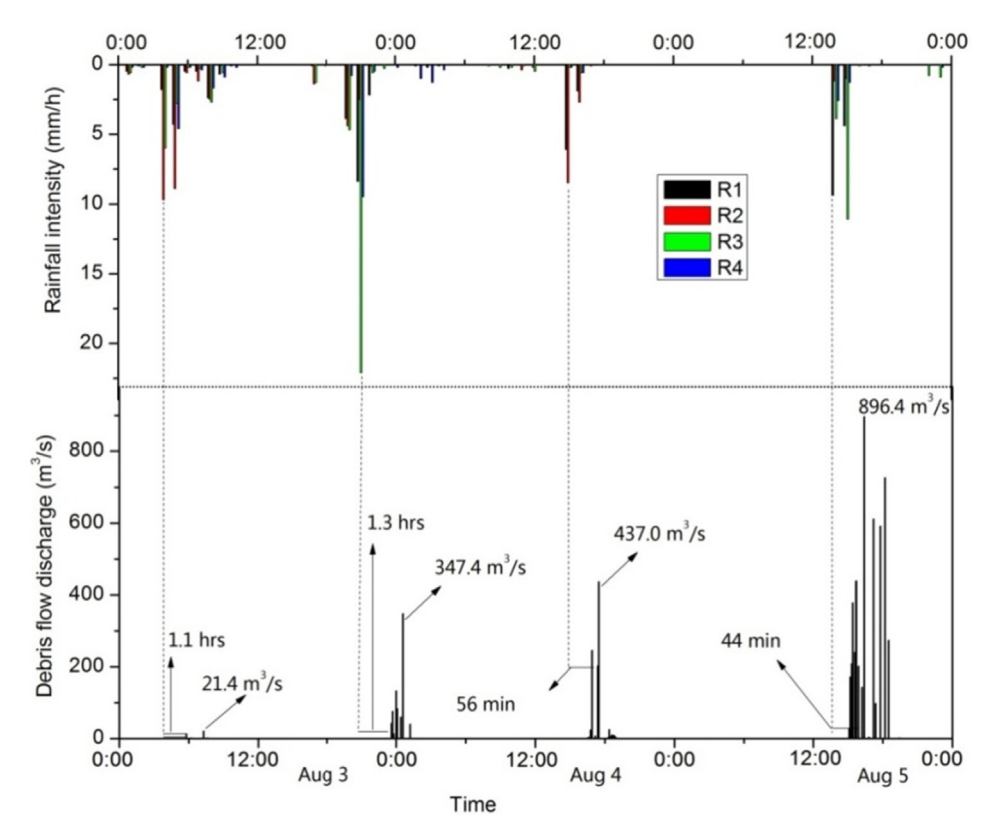


Fig. 14. Rainfall and debris flow processes on August 3-5, 2008.

and 62 separate surges.

The first rainfall peak with an average amount of 11.8 mm was distributed uniformly across the watershed during 03:15–05:30, and the first debris flow event occurred at 06:30 on July 24, approximately 1.7 h after the peak 10-min rainfall. The initial several surge discharges were small (that is, 2.0–9.5 m³/s); however, the peak discharge of 272.7 m³/s that appeared at 07:34—the fourteenth surge—indicated the breaking of a small blockage body.

The second debris flow event was monitored at 03:53 on July 25, approximately 1.3 h after the rainfall peak. The initial several discharges were large (greater than200  $\rm m^3/s$ ) and the peak discharge was 1358.3  $\rm m^3/s$ . The third event was monitored at 14:24 on July 25, approximately 0.4 h after the rainfall peak. Although this lag was reasonably short, the first discharge of 2262.5  $\rm m^3/s$  and the following surges with relatively large discharges indicated that repeated breaking of blockages was the mechanism of debris flow formation.

Another event occurred on August 3–5, 2008 (Fig. 14). The rainfall began at 00:18 am on August 3, but with very low intensity observed at all four rain gauges. The first peak appeared at 04:40 at R2 with 18.6 mm of rainfall in the following 1.2 h to 05:58. The rainfall amount at R2 was much higher than at the other three gauges, which recorded values no greater than 8.0 mm. This suggests the first small debris flow, which was monitored at 04:50 and comprised five surges with peak discharge of 21.4 m³/s, was induced by the rainfall in tributary II during 04:40–5:58. This is representative of a normal hydrological condition in that both the time lag and the peak discharge were reasonable.

The second debris flow was monitored approximately 15 h after the first ended (that is, at 22:35 on August 3). From Fig. 14, it can be seen that the first surge was monitored approximately 1.3 h after the rainfall peak of 22.1 mm during 20:50–21:38; the time lag was estimated at 1.3 h according to the 10-min rainfall process. The discharge of the first six surges was small, that is, no more than 132.9  $\rm m^3/s$ ; however, the seventh surge with discharge of 347.3  $\rm m^3/s$  was indicative of dam

blocking. This debris flow lasted for 3.4 h and comprised 12 surges. It was most likely to have originated following the rainfall in tributary III because of the higher volume in this tributary compared with the others.

The third rainfall peak was recorded at R1 and R2 with rainfall of 11.2 and 8.0 mm, respectively, during 14:10–15:20 on August 4, which suggests that the debris flow was initiated by the rainfall in tributary I. The debris flow was monitored 56 min later. The peak discharge was  $437.0~{\rm m}^3/{\rm s}$  and it occurred at 16:27, that is, approximately 2 h after the rainfall peak. This indicates that the runoff accumulation took some time to break the dam and increase the discharge. This debris flow comprises 22 surges and it persisted for 3.4 h. After the peak surge, the following surges were relatively small, that is, no greater than 25.4  ${\rm m}^3/{\rm s}$ . Therefore, we inferred that the blockage body failed entirely before 16:27 and that the following surges were formed from residual soil materials.

The fourth debris flow occurred on August 5, approximately 20 h after the end of the third debris flow. The rainfall began at 13:22 at R1 and was subsequently concentrated over R1 and R3 during a 2-h period with rainfall amounts of 13.8 and 15.0 mm, respectively. The debris flow was monitored approximately 44 min after the peak rainfall, and except for the initial several surges, the discharge of the surges was reasonably large (peak discharge: 896.4  $\rm m^3/s$ ), which indicates the existence of the blockage–breaking effect. Notably, the blockage–breaking process might not have occurred just once but could have continued repeatedly, which would have resulted in the sequence of large discharges.

#### 5.2. Debris flow hydrographs and formation mechanism

A flow hydrograph is a natural indicator of the hydrological process because it is representative of the system's ultimate behavior. A normal water flow hydrograph generally has a continuous normal distribution shape with one or multiple peaks (Fig. 15a); however, the debris flow

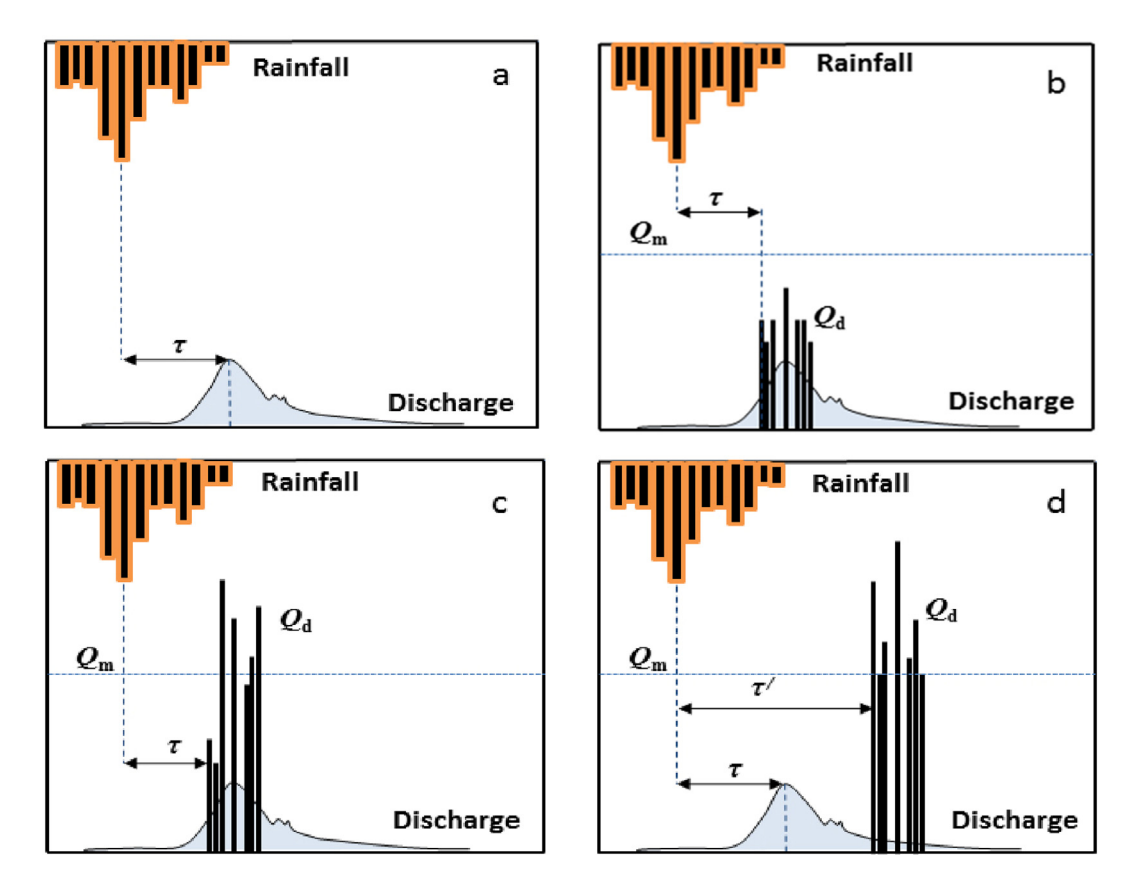


Fig. 15. Debris flow hydrograph modes related to time lag and discharge ( $\tau$  represents the normal time lag from the triggering rainfall to the debris flow occurrence;  $\tau'$  represents the abnormal time lag;  $Q_m$  represents the potential maximum debris flow discharge and  $Q_d$  is the real debris flow discharge).

hydrographs here present an intermittent saw-tooth shape. Analysis of the discharge hydrographs of all 36 events in this watershed showed that the normal  $\tau$  is  $\leq 1$  h and  $\varUpsilon \leq 3.3$ . The effect of the ratio  $\varUpsilon$  is approximately equivalent to the peak discharge  $Q_{\rm max}$ , which is more directly obtained through observations. In this case,  $Q_{\rm max}$  is approximately 250 m³/s, and the hydrographs could be classified into three types.

- a. Time lag  $\tau$  is in a normal range and discharge  $Q_d$  is consistently below the upper limit of the debris flow capacity  $Q_m$  (Fig. 15b).
- b. Time lag  $\tau$  is in a normal range and discharge  $Q_{\rm d}$  is higher than the upper limit of the debris flow capacity  $Q_{\rm m}$  (Fig. 15c).
- c. Time lag  $\tau$  is longer than the normal range and discharge  $Q_{\rm d}$  is consistently higher than the upper limit of the debris flow capacity  $Q_{\rm m}$  (Fig. 15d).

Undoubtedly, variation of rainfall is the first causative factor of intermittency. It determines the most likely potential source regions of material for the debris flows, and it not only differs spatially but also temporally. The cycle of rainfall peaks could maintain the duration of a debris flow, while the interval between peaks would determine the intermittency of the surges; otherwise, the coincident appearance of widespread high-intensity rainfall over a source area could produce high volumes of sediment irrespective of the material types.

A debris flow acts as a normal hydrological process or presents an abnormal appearance. Debris flows presenting normal characteristic parameters are formed as a mixture of the normal water flood and the instantaneous soil supply, derived from either intermittent slope failure and/or channel failure. The surges are formed because of the randomness of the slope failures. Even under uniform rainfall, failure processes are intermittent, spatially varied and of varying magnitude, according to in situ experiments on a slope in the source region (Guo

et al., 2016a). Given that the process of source soil supply is rarely seen, experiments that have revealed the randomness of the slope failure process have also indicated that it can be considered a stochastic sequence. The mechanism behind this randomness is attributable both to the heterogeneity of the soil properties (for example, grain composition) and to the uneven slope properties (for example, microtopography and soils) on the catchment scale (Guo et al., 2016a).

Abnormal debris flows involve blockage–breaking phenomena and do not show a "water-dominated" characteristic. The large failures that lead to channel blocking and runoff accumulation, which trigger the blockage–breaking effect, act as the key factor in the formation of debris flow surges in the main channel. These extraordinary events thus disturb and then reconstruct the underlying hydrological processes. The accumulation time and outburst flow amount depend on many factors that include the amount and properties of the failure bodies, failure location and local channel conditions. The blockage–breaking process could occur as a one-off event or as a repeated sequence. The randomness behind the entire process is the reason for the variation in the characteristics of the debris flows (such as time, hydrograph and properties) within a watershed. This highlights the effect of material supplies in the process of debris flow formation.

#### 5.3. Rainfall conditions for debris flow formation

In most cases, the debris flows were triggered corresponding to a specific sudden increase in rainfall, which allowed us to determine the rainfall responsible for debris flow initiation (and/or slope failure). Rainfall conditions are generally analyzed based on *I-D* thresholds (or using other models based on rainfall parameters) that rely on historical data (for example, Caine, 1980; Guzzetti et al., 2007, 2008; Guo et al., 2016b, 2016c). Moreover, the runoff condition for debris flow initiation in the type of catchment considered in this study is generally defined as

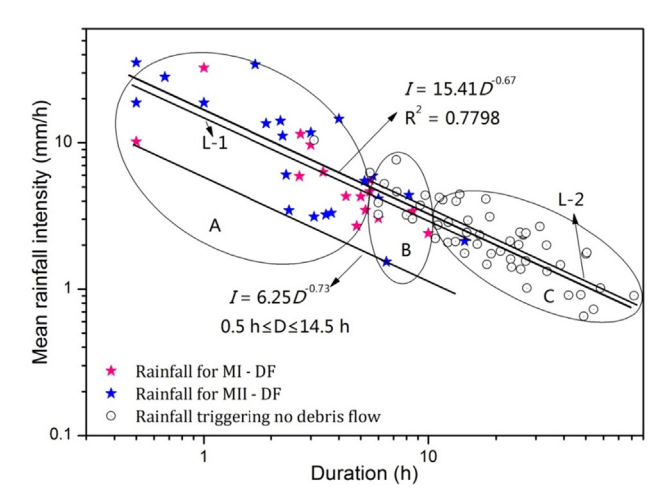


Fig. 16. I-D relations of rainfall amounts and thresholds for debris flows.

a specific surface water runoff discharge threshold required for initiating debris flows from sediment within channels (for example, Takahashi 1991, 2007; Tognacca et al., 2000; Gregoretti, 2000; Gregoretti and Fontana, 2008; Coe et al., 2008; Rosatti et al., 2019). Considering the reasonably low runoff required for debris flow initiation in the tributaries (such as the spring water shown in Fig. 3), this runoff threshold appears senseless. In this study, we analyzed the rainfall conditions required for debris flow initiation, not only to propose the threshold but also to suggest coupling of the water and soil characteristics.

In addition to the rainfall events that triggered debris flows, another 71 events with considerable rainfall amounts, which occurred during 2007-2017 but did not trigger debris flows, were selected for comparison purposes. The selected events mainly had total rainfall amounts > 20 mm and the maximum value was 90.1 mm. The corresponding I-D relations shown in Fig. 16 indicate the following. (1) The total rainfall amount is not the key triggering factor, that is, debris flows can occur following rainfall with a total amount of < 10 mm, and most of the "big" rainfall events with abundant amounts have duration > 6 h. (2) The general tendency of the I-D relation of all rainfall events can be expressed as a uniform relation:  $I = 15.41 D^{-0.67}$ , and the tendencies of the rainfall events that either trigger or do not trigger debris flows are close (L-1 and L-2 in Fig. 16). However, debris flows did not necessarily occur during the big rainfall events with long duration; instead, they were more likely triggered during events that lasted no longer than 10 h. For example, five and eight events were triggered by rainfall lasting < 1 and < 2 h, respectively. Statistics show that 31/36 (86%) of the rainfall events that triggered debris flows lasting < 6 h. (3) The rainfall conditions suitable for normal and abnormal debris flows are similar. This finding indicates that big events (such as landslides) and shallow slope failures require similar amounts of rainfall in the various source regions. The total rainfall threshold can be expressed as  $I=6.25~D^{-0.73}$  (0.5  $\leq D \leq$  14.5 h), that is, as the lowest line of rainfall able to trigger debris flows shown in Fig. 16.

Based on the above analysis and the duration identification by meteorological departments (China Meteorological Administration, 2005), the rainfall can be separated into three categories.

- 1) Short duration (0–6 h) with high mean intensity (2.7–35.4 mm/h). This type of rainfall is highly prone to triggering debris flows, that is, almost all the rainfall events of this type triggered debris flows (except one case, as shown in Ellipse A in Fig. 16).
- 2) Medium duration (6–12 h) with medium mean intensity (1.5–4.4 mm/h). Debris flows occurred in 7 of the 16 (44%) events with this type of rainfall; thus, this rainfall type is also highly prone to triggering debris flows (Ellipse B in Fig. 16).

3) Long-duration (greater than12 h) with low mean intensity (0.7–4.1 mm/h). Although this type of event always produces a remarkable amount of rainfall (max.: 90.1 mm, min.: 50.9 mm and mean: 56.9 mm), debris flows were rarely triggered (Ellipse C in Fig. 16).

#### 6. Discussion

The target area in this study is well known for its active debris flows and its long-term monitoring history. Many previous studies have investigated the characteristics of the debris flows in this area (for example, Li et al., 2003, 2004; Liu et al., 2008; 2009) as well as the rainfall conditions (Cui et al., 2007; Guo et al., 2013). However, none of the earlier research has investigated the debris flow formation processes and related environmental conditions. Research has revealed that fluid instability and roll waves of debris flows produce the separation of flow and lead to surge appearance (Weir, 1982; Ng and Mei, 1994; Wan and Wang, 1994; Hungr, 2000). However, such work has generally originated from the perspective of flow movement and focused on a mature debris flow body, rather than considering formation processes at the watershed scale.

This work investigated the conditions of material supply in the source regions and distinguished debris flow formation processes from the hydrological perspective using two key indices ( $\tau$  and Q), which are generally used to represent the runoff yield and influx processes. A semi-quantitative hydrological simulation was conducted to investigate the water runoff discharge during debris flow events. Although the results were not validated by the hydrographs because of a lack of data on real water flow discharge, which is nearly impossible to measure during debris flow events, the hydrological process-based framework is recommended because it provides a reference for the runoff condition for debris flows (Gregoretti and Fontana, 2008; Wei et al., 2018; Pastorello et al., 2020). The objective of this work was not to perform a detailed numerical simulation of debris flow initiation and propagation, but to provide an estimation of catchment response in terms of discharge at a reference section. Although the formation of debris flows was presented based on a preliminary theoretical framework, the length of the analyzed data series corroborates the results. It was established that debris flows are potentially formed by instantaneous mixing of shallow failures or by abrupt breaking of blockages and that they present different hydrological consequences. We also found that the rainfall conditions required for the formation of different types of debris flow are similar.

The interpretative scheme of debris flow formation processes relies on conjecture based on the corresponding relations between rainfall and flow discharge, which are regarded as the input and output of a system, respectively. Actual observations of debris flow initiation, either in relation to mass failure along a sliding surface or concentrated runoff within a steep channel in the headwater regions, were missing. These measurements are difficult to obtain because of the harsh field conditions in the source regions (for example, very steep slopes, high relief, fractured bedrocks, rockfalls and limited space for device installation). In comparison with other catchments in which physical monitoring has been realized, for example, Chalk Cliffs, Gadria, Illgraben, Rebaixader and others (Berger et al., 2011; McCoy et al., 2012; Kean et al., 2013; Comiti et al., 2014; Hürlimann et al., 2014, 2019; Walter et al., 2017; Coviello et al., 2019), the scale of the watershed in this study is much larger and the material sources are more diverse and distributed more randomly. Therefore, monitoring is much more complex. In future work, targeted monitoring will be a primary objective using an integrated approach combining equipment such as piezometers, erosion probes, geophones and video cameras. However, it must be emphasized that even with increased monitoring of headwater regions, a knowledge gap will remain between the occurrence of slope failures in the source region and the appearance of mature debris flows at the outlet, including the confluence and propagation processes.

X. Guo, et al. Journal of Hydrology 589 (2020) 125184

Therefore, a logical theoretical framework and some conjecture will still be required to a certain extent.

The time and type of debris flow initiation in the source regions present significant uncertainties that can affect the reliability of the formation process and the threshold. Inappropriate selection of the initiation time can result in an incorrect duration (*D*) and a consequent non-significant or non-representative average intensity (*I*). Moreover, the rainfall responsible for the occurrence of landslides and debris flows differs. The different supply types affect not only the magnitude but also the propagation process of debris flows, which ultimately result in the differences between normal and abnormal phenomena. We admit that the identifications performed in this work relied somewhat on experience. However, this is difficult to avoid given the current circumstances, primarily because of the difficulties associated with monitoring debris flow initiation in the headwater region.

Given the uncertainty that exists in terms of data monitoring and data processing, we have been unable to quantify the errors in our data or to verify this uncertainty. Nevertheless, based on the known facts, despite the natural inhomogeneity and randomness, which play an important part in surge formation, we consider our monitored data of the case studies sufficiently reliable.

#### 7. Conclusions

The rainfall events responsible for 36 debris flows during 2006–2017 were identified both spatially and temporally and the hydrographs of the debris flow discharge of these events were analyzed based on the relations between the debris flows and rainfall. The intermittent saw-tooth shaped hydrographs of the presented debris flows differ from the shape of a continuous normal distribution hydrograph of water flow discharge. On the basis of the two key hydrological parameters, the time lag  $(\tau)$  between debris flow occurrence and peak rainfall and the ratio of debris flow discharge to water flow discharge  $(\Upsilon)$ , the debris flows were considered as either normal or abnormal hydrological processes. We suggest that normal debris flows formed when shallow slope failures mixed immediately with channel runoff, whereas abnormal debris flows formed following the channel blockage—breaking effect in the headwater region.

The rainfall threshold for debris flow initiation was proposed as  $I=6.25\,D^{-0.73}$  (0.5  $\leq D \leq$  14.5 h). Debris flows were related more to rainfall pattern than to rainfall amount, that is, most occurred within 6 h of a rainfall event with high mean intensity and short duration. However, the formation type, process and discharge of the debris flows showed no direct relationship with rainfall amount.

This research elucidated the uncertainty and randomness associated with all the above processes. Based on the conceptual framework that a debris flow is the product of a rainfall-induced hydrological process involving the supply of soil materials, we determined that rainfall variation causes intermittency of the soil supply and uncertainty regarding its location and scale. The modalities of the involvement of soil supply, which might disturb or reorganize the hydrological process, lead to the various debris flow appearances as the system outputs, which are also difficult to predict. This highlights the significance of soil supplies both to debris flow formation and to surge complexity.

#### CRediT authorship contribution statement

Xiaojun Guo: Conceptualization, Data curation, Investigation, Writing - original draft Writing - review & editing. Yong Li: Conceptualization, Writing - review & editing. Peng Cui: Conceptualization. Hua Yan: Data curation. Jianqi Zhuang: Writing - review & editing.

#### **Declaration of Competing Interest**

The authors declare that they have no known competing financial interests or personal relationships that could have appeared to influence the work reported in this paper.

#### Acknowledgements

This study was supported by the Strategy project, Chinese Academy of Sciences (XDA23090202), National Research and Development Program, China (2017YFC1502504), International project (2016YFE0122400) and NSFC, China (41977257), Department of Land and Resources Project of Sichuan Province (KJ-2018-22) and Western Light of Young Scholars, Chinese Academy of Sciences.

We thank James Buxton and Andrew Stow from Liwen Bianji, Edanz Group China (www.liwenbianji.cn./ac), for editing the English text of a draft of this manuscript.

#### References

- Bardou, E., Jaboyedoff, M., 2008. Debris flows as a factor of hillslope evolution controlled by a continuous or a pulse process? Geol. Soc. Spec. Pub. 296, 63–78.
- Berger, C., McArdell, B.W., Schlunegger, F., 2011. Direct measurement of channel erosion by debris flows, Illgraben, Switzerland. J. Geophys. Res. 116 (F1), F01002.
- Caine, N., 1980. The rainfall intensity-duration control of shallow landslides and debris flows. Geografiska Annaler. Series A. Phys. Geogr. 62, 23–27.
- Capra, L., Coviello, V., Borselli, L., Márquez-Ramírez, V.-H., Arámbula-Mendoza, R., 2018. Hydrological control of large hurricane-induced lahars: evidences from rainfall, seismic and video monitoring. Nat. Hazards Earth Syst. Sci. 18, 781–794.
- Chen, J., He, Y.P., Wei, F.Q., 2005. Debris flow erosion and deposition in Jiangjia Gully, Yunnan, China. Environ. Geol. 48, 771–777.
- Chen, K.T., Chen, X.Q., Niu, Z.P., Guo, X.J., 2019. Early identification of river blocking induced by tributary debris flow based on dimensionless volume index. Landslides 16, 2335–2352.
- China Meteorological Administration, 2005. Short-term weather forecast quality inspection methods. In: Meteorological and regulations compilation of the PRC (2005).
- Coe, J.A., Glancy, P.A., Whitney, J.W., 1997. Volumetric analysis and hydrologic characterization of a modern debris flow near Yucca Mountain Nevada. Geomorphology 20, 11–28.
- Coe, J.A., Kinner, D.A., Godt, J.W., 2008. Initiation conditions for debris flows generated by runoff at Chalk Cliffs, central Colorado. Geomorphology 96 (3–4), 270–297.
- Comiti, F., Marchi, L., Macconi, P., Arattano, M., Bertoldi, G., Borga, M., Brardinoni, F., Cavalli, M., D'Agostino, V., Penna, D., Theule, J., 2014. A new monitoring station for debris flows in the European Alps: first observations in the Gadria basin. Nat. Hazards 73 (3), 1175–1198.
- Coviello, V., Arattano, M., Comiti, F., Macconi, P., Marchi, L., 2019. Seismic characterization of debris flows: insights into energy radiation and implications for warning. J. Geophys. Res. Earth Surface 1–24.
- Cui, P., Chen, X.P., Wang, Y.Y., Hu, K.H., Li, Y., 2005. Jiangjia Ravine debris flows in the southwestern China. In: Jakob, M., Hungr, O. (Eds.), Debris-flow Hazards and Related Phenomena. Springer-Verlag, pp. 565–594.
- Cui, P., Guo, X.J., Yan, Y., Li, Y., Ge, Y.G., 2018. Real-time observation of an active debris flow watershed in the Wenchuan Earthquake area. Geomorphology 321 (15), 153–166.
- Cui, P., Zhou, G.G., Zhu, X.H., Zhang, J.Q., 2013. Scale amplification of natural debris flows caused by cascading landslide dam failures. Geomorphology 182, 173–189.
- Cui, P., Zhu, Y.Y., Chen, J., Han, Y.S., Liu, H.J., 2007. Relationships between antecedent rainfall and debris flows in Jiangjia Ravine, China. In: Chen, C.L., Major, J.J. (Eds.), Debris-flow Hazard Mitigation-Mechanics, Prediction, and Assessment. Millpress, Rotterdam, pp. 1–10.
- Dal Sasso, S.F., Sole, A., Pascale, S., Sdao, F., Bateman Pinzòn, A., Medina, V., 2014. Assessment methodology for the prediction of landslide dam hazard. Nat. Hazards Earth Syst. Sci. 14, 557–567.
- Davies, T.R., 1986. Large debris flows: a macroviscous phenomenon. Acta Mech. 63, 161–178.
- Davies, T.R., 1990. Debris flow surges experimental simulation. New Zealand J. Hydrol. 29, 18–46.
- Fan, X.M., Rossiter, D.G., Westen, C.J.V., Xu, Q., Görüm, T., 2014. Empirical prediction of coseismic landslide dam formation. Earth Surf. Proc. Land. 39 (14), 1913–1926.
- Godt, J.W., Coe, J.A., 2007. Alpine debris flows triggered by a 28 July 1999 thunderstorm in the central Front Range, Colorado. Geomorphology 84 (1–2), 80–97.
- Gregoretti, C., 2000. The initiation of debris flow at high slopes: experimental results. J. Hydraul. Res. 38 (2), 83–88.
- Gregoretti, C., Fontana, G.D., 2008. The triggering of debris flow due to channel-bed failure in some alpine headwater basins of the Dolomites: analyses of critical runoff. Hydrol. Process. 22 (13), 2248–2263.
- Griffiths, P.G., Webb, R.H., Melis, T.S., 2004. Frequency and initiation of debris flows in Grand Canyon, Arizona. J. Geophys. Res. 109, F04002.
- Guo, X.J., Cui, P., Li, Y., 2013. Debris flow warning threshold based on antecedent

- rainfall: a case study in Jiangjia Ravine, Yunnan, China. J. Mountain Sci. 10 (2), 305–314.
- Guo, X.J., Li, Y., Cui, P., 2016a. Discontinuous slope failures and pore-water pressure variation. J. Mountain Sci. 13 (1), 116–125.
- Guo, X.J., Cui, P., Li, Y., Zou, Q., Kong, Y.D., 2016b. The formation and development of debris flows in large watersheds after the 2008 Wenchuan Earthquake. Landslides 13 (1), 25–37.
- Guo, X.J., Cui, P., Li, Y., Fan, J.L., Yan, Y., Ge, Y.G., 2016c. Temporal differentiation of rainfall thresholds for debris flows in Wenchuan earthquake-affected areas. Environ. Earth Sci. 75 (2), 1–12.
- Guo, X.J., Cui, P., Marchi, L., Ge, Y.G., 2017. Characteristics of rainfall responsible for debris flows in Wenchuan Earthquake area. Environ. Earth Sci. 76, 596.
- Guzzetti, F., Peruccacci, S., Rossi, M., Stark, C., 2007. Rainfall thresholds for the initiation of landslides in central and southern Europe. Meteorol. Atmos. Phys. 98, 239–267.
- Guzzetti, F., Peruccacci, S., Rossi, M., Stark, C., 2008. The rainfall intensity-duration control of shallow landslides and debris flows. an update. Landslides 5, 3–17.
- Hallerberg, S., Altmann, E.G., Holstein, D., Kantz, H., 2007. Precursors of extreme increments. Phys. Rev. E 75, 016706.
- Hungr, O., 2000. Analysis of debris flow surges using the theory of uniformly progressive flow. Earth Surface Progress. Landforms 25, 483–495.
- Hürlimann, M., Abancó, C., Moya, J., Vilajosana, I., 2014. Results and experiences gathered at the Rebaixader debris-flow monitoring site, Central Pyrenees, Spain. Landslides 11 (6), 939–953.
- Hürlimann, M., Coviello, V., Bel, C., Guo, X., Berti, M., Graf, C., Hübl, J., Miyata, S., Smith, J.B., Yin, H.Y., 2019. Debris-flow monitoring and warning: Review and examples. Earth Sci. Rev. 199, 102981.
- Iadanza, C., Trigila, A., Napolitano, F., 2016. Identification and characterization of rainfall events responsible for triggering of debris flows and shallow landslides. J. Hydrol. 541, 230–245.
- Iverson, R.M., Reid, M.E., LaHusen, R.G., 1997. Debris-flow mobilization from landslides Annu. Rev. Earth Planet. Sci. 25, 85–138.
- Iverson, R.M., Reid, M.E., Iverson, N.R., LaHusen, R.G., Logan, M., Mann, J.E., Brien, D.L., 2000. Acute sensitivity of landslide rates to initial soil porosity. Science 290, 513–516.
- Kang, Z.C., Cui, P., Wei, F.Q., He, S.F., 2006. Observation Data of Debris Flows in Jiangjia Gully, Yunnan. Beijing Science Press, Beijing (in Chinese).
- Kean, J.W., McCoy, S.W., Tucker, G.E., Staley, D.M., Coe, J.A., 2013. Runoff-generated debris flows: Observations and modeling of surge initiation, magnitude, and frequency. J. Geophys. Res. Earth Surf. 118 (4).
- Li, Y., Yao, S.F., Hu, K.H., Chen, X.Q., Cui, P., 2003. Surges and deposits of debris flow in Jiangiia Gully. J. Mountain Sci. 21 (6), 712–715.
- Li, Y., Hu, K.H., Yue, Z.Q., Tham, T.G., 2004. Termination and deposition of debris-flow surge. Landslides: Evaluation and Stabilization. Taylor & Francis Group, London, 1451–1456.
- Li, Y., Su, P.C., Cui, P., Hu, K.H., 2008. A probabilistic view of debris flow. J. Mountain Sci. 5 (2). 91–97.
- Liu, J.J., Li, Y., Su, P.C., Cheng, Z.L., 2008. Magnitude–frequency relations in debris flow. Environ. Geol. 55 (6), 1345–1354.
- Liu, J.J., Li, Y., Su, P.C., Cheng, Z.L., Cui, P., 2009. Temporal variation of intermittent surges of debris flow. J. Hydrol. 365 (3–4), 322–328.
- Lumbroso, D., Gaume, Eric, 2012. Reducing the uncertainty in indirect estimates of extreme flash flood discharges. J. Hydrol. 414–415, 16–30.
- Marchi, L., Arattano, M., Deganutti, A.M., 2002. Ten years of debris-flow monitoring in the Moscardo Torrent (Italian Alps). Geomorphology 46 (1), 1–17.

- McArdell, B.W., Bartelt, P., Kowalski, J., 2007. Field observations of basal forces and fluid pore pressure in a debris flow. Geophys. Res. Lett. 34 (7), 248–265.
- McCoy, S., Kean, J., Coe, J., Tucker, G., Staley, D., Wasklewicz, T., 2012. Sediment entrainment by debris flows: In situ measurements from the headwaters of a steep catchment. J. Geophys. Res. Earth Surf. 117 (F3), F03016.
- Mishra, S.K., Singh, V.P., 2003. Soil conservation service curve number (SCS-CN) Methodology. Kluwer Academic Publishers, Dordrecht, The Netherland, pp. 2003.
- Navratil, O., Liébault, F., Bellot, H., Travaglini, E., Theule, J., Chambon, G., Laigle, D., 2013. High-frequency monitoring of debris-flow propagation along the Réal Torrent, Southern French Alps. Geomorphology 201, 157–171.
- Ng, C.O., Mei, C.C., 1994. Roll waves on a shallow layer of mud modelled as a power-law fluid. J. Fluid Mech. 263 (-1), 151–184.
- Nikolopoulos, E.I., Crema, S., Marchi, L., Marra, F., Guzzetti, F., Borga, M., 2014. Impact of uncertainty in rainfall estimation on the identification of rainfall thresholds for debris flow occurrence. Geomorphology 221 (11), 286–297.
- Nikolopoulos, E.I., Borga, M., Creutin, J.D., Marra, F., 2015. Estimation of debris flow triggering rainfall: Influence of rain gauge density and interpolation methods. Geomorphology 243, 40–50.
- Pastorello, R., D'Agostino, V., Hürlimann, M. Debris flow triggering characterization through a comparative analysis among different mountain catchments. Catena. 196: 104348.
- Reid, M.E., Nielsen, H.P., Dreiss, S.J., 1988. Hydrologic factors triggering a shallow hillslope failure. Bull. Assoc. Eng. Geol. 25 (3), 349–361.
- Rosatti, G., Zugliani, D., Pirulli, M., Martinengo, M., 2019. A new method for evaluating stony debris flow rainfall thresholds: the Backward Dynamical Approach. Helliyon 5,
- SCS. 1985. Hydrology. National Engineering Handbook, Soil Conservation Service. USDA, Washington, DC.
- Takahashi, T., 1991. Debris flow. Monograph of IAHR. AA Balkema Rotterdam. Takahashi, T., 2007. Debris Flow. CRC Press.
- Tognacca, C., Bezzola, G. R., Minor, H. E., 2000. Threshold criterion for debris flow initiation due to channel bed failure, In: Wieczoreck, G. F., (Eds.), Proceedings of the Second International Conference on Debris Flow Hazards Mitigation, Taipei, Springer.
- Theule, J.I., Crema, S., Marchi, L., Cavalli, M., Comiti, F., 2018. Exploiting LSPIV to assess debris-flow velocities in the field. Nat. Hazard. Earth Syst. Sci. 18, 1–13.
- Walter, F., Burtin, A., McArdell, B., Hovius, N., Weder, B., Turowski, J., 2017. Testing seismic amplitude source location for fast debris-flow detection at Illgraben, Switzerland. Nat. Hazards Earth Syst. Sci. 17 (6), 939–955.
- Wan, Z.H., Wang, Z.Y., 1994. Hyperconcentrated Flow. IAHR Publication, pp. 290.
  Wei, Z.L., Xu, Y.P., Sun, H.U., Xie, W., Wu, G., 2018. Predicting the occurrence of channelized debris flow by an integrated cascading model: A case study of a small debris flow-prone catchment in Zhejiang Province, China. Geomorphology 308, 78–90.
- Weir, G.J., 1982. Kinematic wave theory for Ruapehu lahars. NZ J. Sci. 25, 197–203.
  Wu, J.S., Kang, Z.C., 1993. Observation Researches on Debris Flows in Jiangjia Gully Yunnan. Science Press, Beijing, pp. 235 (in Chinese).
- Zhou, G.G.D., Cui, P., Chen, H.Y., Zhu, X.H., Tang, J.B., Sun, Q.C., 2013. Experimental study on cascading landslide dam failures by upstream flows. Landslides 10 (5), 633–643.
- Zhou, G.G.D., Cui, P., Zhu, X.H., Chen, H.Y., Sun, Q.C., 2015. A preliminary study of the failure mechanisms of cascading landslide dams caused by upstream flows. Int. J. Sedim. Res. 30 (3), 223–234.